MULTIPLE WINDOW DETECTORS

A THESIS SUBMITTED TO
THE GRADUATE SCHOOL OF NATURAL AND APPLIED SCIENCES
OF
MIDDLE EAST TECHNICAL UNIVERSITY

BY

OKTAY SİPAHİGİL

IN PARTIAL FULFILLMENT OF THE REQUIREMENTS
FOR
THE DEGREE OF MASTER OF SCIENCE
IN
ELECTRICAL AND ELECTRONICS ENGINEERING

SEPTEMBER 2010

Approval of the thesis:

MULTIPLE WINDOW DETECTORS

submitted by **OKTAY SİPAHİGİL** in partial fulfillment of the requirements for the degree of **Master of Science in Electrical and Electronics Engineering Department, Middle East Technical University** by,

Prof. Dr. Canan Özgen _____
Dean, Graduate School of **Natural and Applied Sciences**

Prof. Dr. İsmet Erkmen _____
Head of Department, **Electrical and Electronics Engineering**

Assoc. Prof. Dr. Tolga Çiloğlu _____
Supervisor, **Electrical and Electronics Engineering Dept., METU**

Examining Committee Members:

Prof. Dr. Mübeccel Demirekler
Electrical and Electronics Engineering Dept., METU _____

Assoc. Prof. Dr. Tolga Çiloğlu
Electrical and Electronics Engineering Dept., METU _____

Prof. Dr. Mustafa Kuzuoğlu
Electrical and Electronics Engineering Dept., METU _____

Assoc. Dr. Çağatay Candan
Electrical and Electronics Engineering Dept., METU _____

Işın Akyıldız (M.Sc.)
ASELSAN _____

Date: _____

I hereby declare that all information in this document has been obtained and presented in accordance with academic rules and ethical conduct. I also declare that, as required by these rules and conduct, I have fully cited and referenced all material and results that are not original to this work.

Name, Last Name: OKTAY SİPAHİGİL

Signature :

ABSTRACT

MULTIPLE WINDOW DETECTORS

Sipahigil, Oktay
M.S., Department of Electrical and Electronics Engineering
Supervisor : Assoc. Prof. Dr. Tolga Çiloğlu

September 2010, 70 pages

Energy or DFT detector using a fixed window size is very efficient when signal start time and duration is matched with that of the window's. However, in the case of unknown signal duration, the performance of this detector decreases. For this scenario, a detector system composed of multiple windows may be preferred. Window sizes of such a system will also be fixed beforehand but they will be different from each other. Therefore, one of the windows will better match the signal duration, giving better detection results. In this study, multiple window detectors are analyzed. Their false alarm and detection probability relations are investigated. Some exact and approximate values are derived for these probabilities. A rule of thumb for the choice of window lengths is suggested for the case of fixed number of windows. Detectors with overlapping window structure are considered for the signals with unknown delay. Simulation results are added for these types of detectors.

Keywords: Multiwindow Detection, Hypothesis Testing

ÖZ

ÇOK PENCERELİ TESPİT SİSTEMLERİ

Sipahigil, Oktay
Yüksek Lisans, Elektrik ve Elektronik Mühendisliği Bölümü
Tez Yöneticisi : Doç. Dr. Tolga Çiloğlu

Eylül 2010, 70 sayfa

Sabit pencere uzunluğu ile çalışan, DFT veya enerji tespit sistemi, sinyalin başlangıç zamanı ve uzunluğu pencereninkilere eşit olduğu zaman verimli çalışmaktadır. Fakat, sinyalin uzunluğunun bilinmediği durumda, tespit sisteminin performansı düşer. Bu durumda birden fazla pencereden oluşan bir tespit sistemi tercih edilebilir. Bu sistemin pencere uzunlukları da daha önceden belirlenir ancak pencereler farklı uzunluklara sahiptir. Bu sayede, pencerelerden bir tanesi büyük oranda sinyal uzunluğu ile eşleşerek daha iyi tespit sonuçları verir. Bu çalışmada çoklu pencere tespit sistemleri incelenmiştir. Yanlış alarm ve tespit olasılıkları arasındaki ilişki araştırılmıştır. Bu olasılıklar için bazı kesin ve yaklaşık değerler elde edilmiştir. Pencere sayısının belirlenmiş olduğu durumda, pencere uzunluklarının seçimi için pratik bir kural önerilmiştir. Bilinmeyen bir gecikmeye sahip sinyaller için örtüşmeli pencere yapısına sahip tespit sistemleri incelenmiştir. Bu tipteki tespit sistemleri için benzetim sonuçları eklenmiştir.

Anahtar Kelimeler: Çok Pencereli Tespit, Hipotez Testi

To My Family

ACKNOWLEDGMENTS

I would like to express my deepest gratitude to my supervisor Assoc. Prof. Dr. Tolga Çiloğlu for his guidance, advice, criticism, encouragements and insight throughout the research.

I would also like to thank Assoc. Prof. Dr. Çağatay Candan. He has made his support available in a number of ways.

Thanks to the examining committee members Prof. Dr. Mübeccel Demirekler, Prof. Dr. Mustafa Kuzuoğlu and Işın Akyıldız for evaluating my work and for their valuable comments.

I would like to express my gratitude to Erdal Mehmetcik for his suggestions and support.

Deepest thanks to my family for their love, trust, understanding, and every kind of support not only throughout my thesis but also throughout my life.

TABLE OF CONTENTS

LIST OF FIGURES

FIGURES

CHAPTER 1

INTRODUCTION

1.1 Introduction

Detection Theory is one of the main branches of signal processing. This branch covers a wide range of topics such as radar/sonar applications, digital communication receivers, image analysis, document authentication and biometrics. The common problem in these areas is to determine whether the signal is present or not. Another concern is to estimate the parameters of the signal and extract some information. In most of the applications, parameter estimation together with detection is essential and they must be performed simultaneously. One common technique is the generalized likelihood ratio test (GLRT) which implements the detection and estimation tasks together and its performance is asymptotically pleasing [1].

Many books were written about this subject. Some remarkable ones are [2, 3, 4, 5, 6, 7, 8, 9, 10]. A concise review has been presented by Levy [10]:

> "The three-volume treatise by Van Trees [2, 3, 4] remains an unavoidable starting point, not only due to its completeness, but because of its outstanding exposition of the signal space formulation of signal detection. However, because of its emphasis on CT problems and on Bayesian detection, additional sources are recommended. The book [5] presents a large number of examples where detection problem symmetries can be exploited for designing UMPI tests. The two-volume book by Kay [6, 7] analyses estimation and detection problems from a digital signal processing view point and contains an excellent discussion of the GLRT. Due to its strong emphasis on fundamental principles, Poor's book [8] is probably closest in style to the present text, but with a stronger Bayesian em-

phasis than adopted here. Finally, Helstrom's book [9], although quite advanced, provides a very balanced treatment of Bayesian and non Bayesian view points."

One of the main applications in detection theory is radar and sonar applications. In these applications, the aim is to gather information about the environment. This aim is achieved passively by just listening the environment or by transmitting a series of pulses and then collecting the returned echoes. These echoes, after being detected and their parameters estimated, give some information about the environment. In radar signal processing, a train of electromagnetic (EM) pulses are sent into the medium (air) and the reflected echoes are analyzed. Similarly, in active sonar signal processing, acoustic pulses are used in underwater medium and similar techniques are used in the analysis of the returned echoes. These are active systems, which means that some signals must be transmitted, this in turn makes the transmitter exposed to hostile action. Other type of sonar systems utilize passive listening of the ambient noise and other noise sources, for instance due to the propeller of a ship. This way, the location of the sonar system is not given away. Signal interception is also an important subject of detection. Some of the areas of interception are reconnaissance, surveillance, and other intelligence gathering activities [11]. In [12], interception of weak signal in non-Gaussian noise is studied. Spectral correlation property of cyclostationary signals is used by the multi-cycle and single-cycle detectors. This method accommodates unknown and changing noise level and interference activity and is superior compared to the radiometer.

A huge amount of studies were done in radar signal processing. In [13], almost 700 references were collected and grouped in different topics such as radar clutter modeling and constant false alarm rate detection.

The main purpose of radar/sonar applications is to detect the presence of targets and extract some information about their parameters. To achieve this, the radar/sonar transmitter sends some predefined signals into the environment and receives the echoes returned from different obstacles and targets in the medium. The predefined signal can be a pure frequency wave or its amplitude, frequency or phase can be modulated [14]. The received echoes from these pulses, most of the time, have different parameters than the original signal due to many factors such as the ambient noise, reverberation effect, Doppler shifts caused by non-stationary targets and/or receivers etc. Hence the receiver side must perform some processing to identify the signal as a returned echo. In this process the parameters of the signal are generally the main concern.

Some important performance affecting parameters are as follows:

Energy: The energy of the transmitted signal, in most cases, will be significantly reduced by the attenuation in the medium. Hence the energy of the returned echo can be drastically reduced.

Envelope shape: The transmitted signal has a predefined envelope shape. Modification of the envelope depends on the environment.

Phase and frequency: When the transmitted signals are tonals, they have phase and frequency parameters. Usually phase is modeled as a random variable uniformly distributed in the interval $[0, 2\pi)$. Transmitted and received signals differ in their frequencies when the relative distance between the target and the receiver/transmitter changes with time. This effect is called as the Doppler effect. Since the observer does not know the relative velocity most of the time, the frequency parameter in the received signal can be modeled as a random variable.

Delay: The initial time of the returning echo depends on the relative location of the target to the transmitter/reciever. Since most of the time the location of that target is not known exactly, this parameter is also modeled as a random variable.

Echo Length: The returned signal length can also be random due to the signal elongation upon reflection. In low resolution radar applications, the difference between the transmitted and received lengths can be insignificant. Therefore, usually detectors are designed for fixed signal lengths, matching the transmitted signal.

The main problem in these applications is to decide if the signal is present in the received echo, when there is full or partial information about the parameters of the returned signal. Different methods are employed to solve this problem. For instance, if the pulse shape is known under additive noise, matched filters are used for maximum detection performance [15], which is also the ”optimal” detector under same specified constraints.

When some parameters are unknown, a frequently used method is the energy detector (“radiometer”) [16], which gives very good results in low SNR cases. The expressions for the

performance of the energy detector is given in [17] when the energy parameter of the signal is modeled as a random variable. Moreover, energy detectors also work when the unknown signals are modeled as samples of a random process [18]. Properties of the energy detector is covered in [19]. However, when SNR values are not low the performance increases by utilizing the fully or partially known parameters. Unknown parameters are estimated before or during the detection process. These estimated values approach to true values when SNR increases [10]. Therefore these methods give better results than the energy detector when SNR is high. The type of detectors differ according to the unknown parameters.

When for instance the frequency of the signal is modeled as random, DFT detectors have near optimum performance. Performance of these detectors are analyzed in [20, 21]. In [22], an optimum detector is derived for the unknown frequency and the performance is compared with other detectors in literature.

In some applications, like counter-measure systems, the receiver may not have the full information about the signal to be detected. In these cases the problem is harder, mainly because there is less information. Even if there are some assumptions about the signal model, there can be multiple possibilities. An extra complexity should be introduced to the detectors to overcome this problem. As an example, for the random length case, one can use multiple window detectors. These multiple window detectors may be composed of energy detectors as in [23]. Another approach for Bayesian detection of a rectangular pulse with unknown duration is developed in [24].

There are also many works on the detection of signals when the noise is modeled as non-Gaussian [25, 26, 27, 28]. In [29] and [30], signal detection under Gaussian noise is performed using higher order statistics. Knowledge of the correlation of noise samples is not needed for the suggested detector to work, and the detector is computationally simple. Optimal methods however depend on the covariance matrix of the noise and the performance of the detector depends on how good the covariance matrix is estimated. In [31], effect of the incorrect estimations are studied.

In a detection problem the performance of the detector is evaluated by its probability of detection and probability of false alarm. These values can be estimated by performing Monte Carlo simulations. If theoretical values can be calculated according to the given signal and noise model, performance values will be known exactly. In calculations of the cumulative dis-

tributions, characteristic functions or moment generating functions are mathematically useful [32, 33]. If the closed forms are too complicated, then approximations may be tried to be found.

1.2 Scope

The aim of this work is to analyze the performances of the detectors suitable for given signal models and to derive and analyze a detector having a good performance in detecting signals with random length.

Signals are modeled as tones with random phase, random frequency and random length. Noise is modeled as white Gaussian. With these models, the detector used to detect random length signals is the multiple window detector. Analytical forms for probability of false alarms are derived and an approximation is made for probability of detection.

All analysis are done in discete domain.

1.3 Outline

Chapter 2 gives definitions of some basic concepts used throughout the work. It introduces the Neyman-Pearson criterion which helps to derive optimal detectors for given signal models. Some properties of the receiver operating characteristic curve is introduced. This curve is used to measure the performance of the detectors.

In Chapter 3, well known and commonly used results for binary hypothesis testing are summarized. In Section 3.2 the signal is modeled as a single sample scalar. In the following sections, complexity of the signal model is increased by adding a new random parameter in each new section.

Chapter 4 is aimed to be the part that is original to this work. In Section 4.2, an approximation is done for the probability of false alarms for the DFT detector used to detect random frequency signals. It is compared with the simulation results. In Section 4.3 detailed analyses are done for multiple window detectors. Their false alarm and detection probabilities are derived. The results of the derivations are compared with the simulation results.

In Chapter 5, simulations are performed for specific scenarios in order to demonstrate some inherent ideas for overlapping multiple windows. In Section 5.1, best window lengths are found for the given example and a general formula is suggested. It is demonstrated that increasing window length increases the performance for that specific example. In Section 5.2, it is shown by simulation that increasing overlap increases the detector performance. In the last section, the detector is composed of both multiple windows and overlaps. For a sequence of signals received continuously in time, detector performances are simulated. Again, increasing overlaps and the number of windows showed an increase in performance.

In Chapter 6, some concluding remarks are made. In addition, this chapter contains some of the future work planned.

CHAPTER 2

REVIEW OF DETECTION CONCEPTS

2.1 Hypothesis Testing

Hypothesis is a set of probability distributions. Commonly, this set is indexed by a set of parameters. A hypothesis is said to be *simple* if it contains a single probability distribution. A hypothesis is said to be *composite* if it contains more than one probability distributions. *Hypothesis testing* is a process of establishing the validity of a hypothesis [34]. If the problem contains two competing hypotheses, then this problem is called binary hypothesis testing problem.

We examine the binary hypothesis testing problem in this work. In this problem, the two hypotheses are named as H_0 and H_1. H_0 is called the *null hypothesis* and H_1 is called the *alternative hypothesis*. In engineering literature, H_0 is the set of distributions belonging to noise data, therefore it is also called *noise only hypothesis*. H_1 is the set of distributions belonging to the summation of signal and noise. This one is also called *signal plus noise hypothesis*.

Let the probability distributions relevant to the problem be parametrized by the parameters in the set $\mathcal{X}$. Now we have a family of probability distributions $\mathcal{M} = \{\Pr_{\mathbf{x}} : \mathbf{x} \in \mathcal{X}\}$. Let $\mathcal{X}_0$ and $\mathcal{X}_1$ be the two disjoint subsets of $\mathcal{X}$. The hypotheses can be formulated as [35].

$$\begin{aligned} H_0 &: \mathbf{x} \in \mathcal{X}_0 \\ H_1 &: \mathbf{x} \in \mathcal{X}_1 \end{aligned} \tag{2.1}$$

The objective is to decide which one is true given some observations.

In the above formulation, $\mathcal{X}_0$ and $\mathcal{X}_1$ are needed to be disjoint, because otherwise, some

distributions would arise in both hypotheses leading to an unsolvable detection problem.

Simple hypothesis testing problem consists of a family of probability distributions $\mathcal{M} = \{\Pr_0, \Pr_1\}$ and the hypotheses can be formulated as

$$\begin{aligned} H_0 &: \Pr_0 \\ H_1 &: \Pr_1 \end{aligned} \tag{2.2}$$

Composite hypothesis testing deals with more than one probability distribution for at least one hypothesis.

The observation vector, that is the result of either H_0 or H_1, is a random vector. Let the observation be $\underset{\sim}{\mathbf{y}}$ taking values on the domain $\mathcal{Y}$. Notationally, the probability density functions corresponding to the parametrized distributions are written as $p_{\underset{\sim}{\mathbf{y}}}(\mathbf{y} \mid \mathbf{x}, H_i)$.

Choosing between the two hypothesis given an observation vector requires a method. This method can be formulized by defining a *decision function* $\mathfrak{d} : \mathcal{Y} \to \{0, 1\}$. Then we can say:

$$\begin{aligned} \mathfrak{d}(\mathbf{y}) = 0 &\Rightarrow \text{ decide } H_0 \\ \mathfrak{d}(\mathbf{y}) = 1 &\Rightarrow \text{ decide } H_1 \end{aligned} \tag{2.3}$$

$\mathfrak{d}$ maps each observation to a hypothesis (by its index). So it partitions $\mathcal{Y}$ into two disjoint sets

$$\mathcal{Y}_i = \{\mathbf{y} : \mathfrak{d}(\mathbf{y}) = i\} \qquad \text{for } i = 0, 1 \tag{2.4}$$

Every disjoint partitioning of $\mathcal{Y}$ into two sets corresponds to a decision function. We can call $\mathbb{D}$ as the set of all decision functions.

The performance of a decision function for the binary hypothesis testing problem is evaluated by two quantities. One is the *probability of detection* (P_{D}) which is the value of the probability of deciding H_1 when it is in fact the correct hypothesis. The other quantity is the *probability of false alarm* (P_{FA}). It is the value of probability of deciding H_1 when the correct hypothesis is H_0. The probability of detection is given as

$$P_{\mathrm{D}}(\mathfrak{d}) = \int_{\mathcal{Y}_1} p_{\underset{\sim}{\mathbf{y}}}(\mathbf{y} \mid H_1) d\mathbf{y} \tag{2.5}$$

and the probability of false alarm is given as

$$P_{\mathrm{FA}}(\mathfrak{d}) = \int_{\mathcal{Y}_1} p_{\underset{\sim}{\mathbf{y}}}(\mathbf{y} \mid H_0) d\mathbf{y} \tag{2.6}$$

The ideal decision function, if it existed, would take decisions such that the resultant probabilities be $P_{\mathrm{D}} = 1$ and $P_{\mathrm{FA}} = 0$. Such a decision function does not exist except in some rare uninteresting cases for example when H_0 always produce 0 and H_1 always produce 1. In this case $\mathfrak{d}(i) = i$ for $i = 0, 1$ does not make any mistake.

What can be done is to choose a $\mathfrak{d} \in \mathbb{D}$ such that P_{D} is as close to 1 and P_{FA} is as close to 0 as possible.

We desire to choose an element of $\mathbb{D}$ which is optimal in some appropriate sense. But, what is optimal depends on the information available. According to the available information, we can list three tests:

- **Bayesian tests** In Bayesian tests, a-priori probabilities are known for the two hypotheses. What is also known is the cost and benefit structure for all the possible outcomes of the test.
- **Minimax tests** In minimax tests, a cost and benefit structure exists but a-priori probabilities are unknown.
- **Neyman-Pearson tests** Only the pdf's of observations under each hypothesis is known in Neyman-Pearson tests.

In this work, a cost structure will not be introduced, therefore only Neyman-Pearson tests will be considered.

2.2 Neyman-Pearson Criterion

Neyman-Pearson philosophy is to choose a test $\mathfrak{d} \in \mathbb{D}$ that maximizes $P_D(\mathfrak{d})$ with the constraint that $P_{\mathrm{FA}}(\mathfrak{d})$ is less than or equal to a constant value.

Let $\mathbb{D}_\alpha = \{\mathfrak{d} \in \mathbb{D} : P_{\mathrm{FA}}(\mathfrak{d}) \leq \alpha\}$. Then,

$$\mathfrak{d}_{NP} = \arg \max_{\mathfrak{d} \in \mathbb{D}_\alpha} P_D(\mathfrak{d}) \tag{2.7}$$

Let

$$L(\mathbf{y}) = \frac{p_{\underset{\sim}{\mathbf{y}}}(\mathbf{y} \mid H_1)}{p_{\underset{\sim}{\mathbf{y}}}(\mathbf{y} \mid H_0)} \tag{2.8}$$

The result of (2.7) is given as

$$\mathfrak{d}(\mathbf{y}) = \begin{cases} 1 & \text{if } L(\mathbf{y}) > \lambda \\ 0 \text{ or } 1 & \text{if } L(\mathbf{y}) = \lambda \\ 0 & \text{if } L(\mathbf{y}) < \lambda \end{cases} \tag{2.9}$$

if the pdf's are continuous, then the probability of occurance of case "$L(\mathbf{y}) = \lambda$" is zero and the threshold λ is the solution to

$$P_{\text{FA}} = \int_{\{\mathbf{y}:L(\mathbf{y})>\lambda\}} p_{\underset{\sim}{\mathbf{y}}}(\mathbf{y} \mid H_0) d\mathbf{y} \tag{2.10}$$

A detailed proof is given in [10].

The test obtained in this sense is called the *likelihood ratio test (LRT)*.

In many cases, taking the logarithm of both sides in the test brings practical advantages in calculations. Using the monotonic increasing property of the logarithm function, the following test is equivalent to the one in (2.9).

$$\mathfrak{d}(\mathbf{y}) = \begin{cases} 1 & \text{if } \ln \mathrm{L}(\mathbf{y}) > \gamma \\ 0 \text{ or } 1 & \text{if } \ln \mathrm{L}(\mathbf{y}) = \gamma \\ 0 & \text{if } \ln \mathrm{L}(\mathbf{y}) < \gamma \end{cases} \tag{2.11}$$

where $\gamma = \ln \lambda$.

2.3 Receiver Operating Characteristic

For all decision functions $\mathfrak{d}$ there is a corresponding pair $(P_{\text{FA}}(\mathfrak{d}), P_{\text{D}}(\mathfrak{d})) \in [0,1] \times [0,1]$. Let $\mathfrak{r} : \mathbb{D} \to [0,1] \times [0,1]$. The set $\mathfrak{r}(\mathbb{D})$ contains all the achievable $(P_{\text{FA}}, P_{\text{D}})$ operating points.

A *receiver operating characteristic* (ROC) is a curve in $[0,1] \times [0,1]$ consisting of different $(P_{\text{FA}}, P_{\text{D}})$ operating points [10]. It can also be called *ROC curve*. The ROC curve of a Neyman-Pearson detector is a curve in $[0,1]\times[0,1]$ consisting of points $(P_{\text{FA}}(\mathfrak{d}_{NP,\alpha}), P_{\text{D}}(\mathfrak{d}_{NP,\alpha}))$ when $P_{\text{FA}} = \alpha$ is swept from 0 to 1. If λ is the LRT threshold, it is swept from 0 to ∞. The

probability of detection and probability of false alarm can be written in terms of λ as

$$P_{\mathrm{D}}(\lambda) = \int_{\lambda}^{\infty} p_{L(\underset{\sim}{\mathbf{y}})}(L(\mathbf{y}) \mid H_1) dL(\mathbf{y})$$
$$P_{\mathrm{FA}}(\lambda) = \int_{\lambda}^{\infty} p_{L(\underset{\sim}{\mathbf{y}})}(L(\mathbf{y}) \mid H_0) dL(\mathbf{y}) \tag{2.12}$$

We can list some properties of a ROC curve for a Neyman-Pearson detector, [10].

1. ROC curve is the upper boundary of the achievable operating points.
2. $(0, 0)$ and $(1, 1)$ are in ROC.
3. $\frac{dP_{\mathrm{D}}}{dP_{\mathrm{FA}}} = \lambda$, where λ is the threshold of the corresponding LRT. Since $\lambda > 0$ for $P_{\mathrm{FA}} > 0$, this statement tells us that in order to increase the probability of detection, one needs to increase the probability of false alarm as well. A critical question to be answered in the detector design process is "which P_{FA} can be tolerated" in the detection problem.
4. ROC curve is concave.
5. $P_{\mathrm{D}} \geq P_{\mathrm{FA}}$ for all points on ROC.

An example of a ROC curve together with all the achievable operating points is given in Figure 2.1.

Proof of 1 This is obvious. For a given P_{FA}, Neyman-Pearson detector gives the highest P_{D} among all the achievable decision functions.

Proof of 2 At the two end points where $\lambda = 0$ and $\lambda = \infty$,

$$P_{\mathrm{D}}(0) = P_{\mathrm{FA}}(0) = 1 \tag{2.13}$$
$$P_{\mathrm{D}}(\infty) = P_{\mathrm{FA}}(\infty) = 0 \tag{2.14}$$

Proof of 3

$$\left.\begin{array}{l} \frac{dP_{\mathrm{D}}}{d\lambda} = -p_{L(\underset{\sim}{\mathbf{y}})}(L(\mathbf{y}) \mid H_1) \\ \frac{dP_{\mathrm{FA}}}{d\lambda} = -p_{L(\underset{\sim}{\mathbf{y}})}(L(\mathbf{y}) \mid H_0) \end{array}\right\} \Rightarrow \frac{dP_{\mathrm{D}}}{dP_{\mathrm{FA}}} = \frac{p_{L(\underset{\sim}{\mathbf{y}})}(L(\mathbf{y}) \mid H_1)}{p_{L(\underset{\sim}{\mathbf{y}})}(L(\mathbf{y}) \mid H_0)} = \lambda \tag{2.15}$$

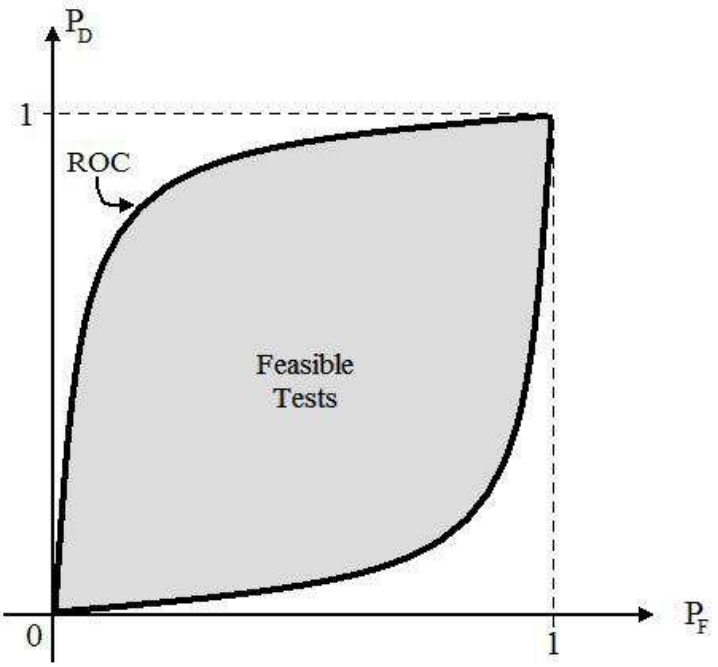

Figure 2.1: Receiver operating characteristic together with all the achievable operating points

Proof of 4 For the proof of 4, the reader may refer to [10].

Proof of 5 Let for $P_{\mathrm{FA}}^{(1)} \geq P_{\mathrm{D}}^{(1)}$, the point $(P_{\mathrm{FA}}^{(1)}, P_{\mathrm{D}}^{(1)})$ be achieved by the decision function $\mathfrak{d}_1$. Then define,

$$\mathfrak{d}_2(\mathbf{y}) = \begin{cases} 1 & \text{if } \mathfrak{d}_1(\mathbf{y}) = 0 \\ 0 & \text{if } \mathfrak{d}_1(\mathbf{y}) = 1 \end{cases} \tag{2.16}$$

With $\mathfrak{d}_2$, the point $(P_{\mathrm{FA}}^{(2)}, P_{\mathrm{D}}^{(2)}) = (P_{\mathrm{D}}^{(1)}, P_{\mathrm{FA}}^{(1)})$ is achievable.

CHAPTER 3

DETECTION OF SIGNALS UNDER NOISE

3.1 Introduction

In this chapter, an attempt is made to develop a consistent notation for the problem of detection of signals under noise. Sections from 3.2 upto 3.8 are discussed in many radar signal processing books such as [10], [7] and [36].

In section 3.6, approximation for detection probability is derived using the DFT detector structure.

In radar applications, usually, the signal length is known. When the length is unknown however, it must be estimated before performing the detection. In section 3.7, such a detector is derived.

3.2 Detection of a Positive Scalar in Gaussian Noise

This section deals with the detection of an unknown constant in Gaussian noise. This case is the one dimensional case of the more general detection problem of known signals in noise. The value of the scalar is unknown to the observer. However, a test independent of the parameter is derived. Since the test will not depend on the parameter, knowing its value is not necessary for the decision function.

Let the signal be defined by its energy parameter, namely

$$s = \sqrt{E} \tag{3.1}$$

where $E \geq 0$ is the energy of the single sample signal.

Let the noise $\underset{\sim}{w}$ be a zero mean Gaussian random variable with variance σ^2.

The observation $\underset{\sim}{y}$ is given in two hypotheses as

$$\begin{aligned} H_0 &: \underset{\sim}{y} = \underset{\sim}{w} \\ H_1 &: \underset{\sim}{y} = s + \underset{\sim}{w} \end{aligned} \tag{3.2}$$

H_0 is a simple hypothesis since it contains only one distribution which is $\mathcal{N}(0, \sigma^2)$. H_1 is composite and it contains a family of distributions $\mathcal{N}(\sqrt{E}, \sigma^2)$ indexed by the parameter E.

$$\begin{aligned} H_0 &= \left\{\mathcal{N}(0, \sigma^2)\right\} \\ H_1 &= \left\{\mathcal{N}(\sqrt{E}, \sigma^2) : E > 0\right\} \end{aligned} \tag{3.3}$$

A short hand notation may be as follows.

$$\begin{aligned} H_0 &: E = 0 \\ H_1 &: E > 0 \end{aligned} \tag{3.4}$$

In order to find the decision function optimum in the Neyman-Pearson sense, one first has to find the likelihood ratio defined as in (2.8). The likelihood ratio can be written as

$$\begin{aligned} \mathrm{L}(y) &= \frac{p_{\underset{\sim}{y}}(y \mid H_1)}{p_{\underset{\sim}{y}}(y \mid H_0)} \\ &= \frac{\frac{1}{\sqrt{2\pi\sigma^2}} \exp\left(-\frac{(y-\sqrt{E})^2}{2\sigma^2}\right)}{\frac{1}{\sqrt{2\pi\sigma^2}} \exp\left(-\frac{y^2}{2\sigma^2}\right)} \\ &= \frac{\frac{1}{\sqrt{2\pi\sigma^2}} \exp\left(-\frac{y^2 - 2\sqrt{E}y + E}{2\sigma^2}\right)}{\frac{1}{\sqrt{2\pi\sigma^2}} \exp\left(-\frac{y^2}{2\sigma^2}\right)} \\ &= \exp\left(\frac{-E}{2\sigma^2}\right) \exp\left(\frac{\sqrt{E}y}{\sigma^2}\right) \end{aligned} \tag{3.5}$$

According to (2.9), the optimum decision function results as 1 if the following is true.

$$\exp\left(\frac{-E}{2\sigma^2}\right) \exp\left(\frac{\sqrt{E}y}{\sigma^2}\right) > \lambda \tag{3.6}$$

where λ is some value.

The test given in (3.6) can be rewritten by using the monotonic increasing property of the logarithm function. Therefore the following is true

$$\ln \mathrm{L}(y) = \frac{-E}{2\sigma^2} + \frac{\sqrt{E}y}{\sigma^2} > \gamma \tag{3.7}$$

where $\gamma = \ln \lambda$.

Decision test using log-likelihood ratio is

$$\begin{aligned} y &> \frac{\sigma^2\gamma}{\sqrt{E}} + \frac{\sqrt{E}}{2} \\ \Rightarrow y &> \tau \end{aligned} \tag{3.8}$$

Threshold of the test τ is defined as $\tau = \frac{\sigma^2\gamma}{\sqrt{E}} + \frac{\sqrt{E}}{2}$. The Neyman-Pearson optimal detector decides H_1 if (3.8) is satisfied. Otherwise it decides H_0.

The threshold value has to be determined from the false alarm constraint of the detector.

The distributions for the random variable $\underset{\sim}{z} = \underset{\sim}{y}$ used in the test is already known for both hypotheses. The probabilities of false alarm and detection can easily be calculated.

$$\begin{aligned} P_{\mathrm{FA}}(\tau) &= \Pr\left\{\underset{\sim}{z} > \tau \mid H_0\right\} \\ &= \int_{\tau}^{\infty} p_{\underset{\sim}{z}}(z \mid H_0)\mathrm{d}z \\ &= \int_{\tau}^{\infty} \frac{1}{\sqrt{2\pi\sigma^2}} \exp\left(-\frac{z^2}{2\sigma^2}\right)\mathrm{d}z \\ &= \int_{\tau/\sigma}^{\infty} \frac{1}{\sqrt{2\pi}} \exp\left(-\frac{z^2}{2}\right)\mathrm{d}z \\ &= \mathrm{Q}\left(\frac{\tau}{\sigma}\right) \end{aligned} \tag{3.9}$$

$$\begin{aligned} P_{\mathrm{D}}(\tau) &= \Pr\left\{\underset{\sim}{z} > \tau \mid H_1\right\} \\ &= \int_{\tau}^{\infty} p_{\underset{\sim}{z}}(z \mid H_1)\mathrm{d}z \\ &= \int_{\tau}^{\infty} \frac{1}{\sqrt{2\pi\sigma^2}} \exp\left(-\frac{(z-\sqrt{E})^2}{2\sigma^2}\right)\mathrm{d}z \\ &= \int_{\frac{\tau-\sqrt{E}}{\sigma}}^{\infty} \frac{1}{\sqrt{2\pi}} \exp\left(-\frac{z^2}{2}\right)\mathrm{d}z \\ &= \mathrm{Q}\left(\frac{\tau}{\sigma} - \frac{\sqrt{E}}{\sigma}\right) \\ &= \mathrm{Q}\left\{\mathrm{Q}^{-1}(P_{\mathrm{FA}}) - \sqrt{\mathrm{SNR}}\right\} \\ &= 1 - \mathrm{Q}\left\{\sqrt{\mathrm{SNR}} - \mathrm{Q}^{-1}(P_{\mathrm{FA}})\right\} \end{aligned} \tag{3.10}$$

where

$$\mathrm{Q}(x) = \frac{1}{\sqrt{2\pi}} \int_x^{\infty} \exp\left(-\frac{u^2}{2}\right) \mathrm{d}u \tag{3.11}$$

is the Gaussian-Q function and

$$\mathrm{SNR} = \frac{E}{\sigma^2} \tag{3.12}$$

is the signal to noise ratio.

Summary The detection problem in this section can be summarized as below.

$$\begin{aligned} H_0 &: \underset{\sim}{y} \sim \mathcal{N}(0, \sigma^2) \\ H_1 &: \underset{\sim}{y} \sim \mathcal{N}(\sqrt{E}, \sigma^2) \end{aligned} \tag{3.13}$$

The decision function that is optimal in the Neyman-Pearson sense:

$$\vartheta_{\mathrm{NP}}(y) = \begin{cases} 1 & \text{if } y > \tau \\ 0 & \text{if } y < \tau \end{cases} \tag{3.14}$$

where

$$\tau = \sigma\, \mathrm{Q}^{-1}(P_{\mathrm{FA}}) \tag{3.15}$$

The ROC curve belonging to ϑ_{NP} is given as

$$P_{\mathrm{D}} = 1 - \mathrm{Q}\left\{ \sqrt{\mathrm{SNR}} - \mathrm{Q}^{-1}(P_{\mathrm{FA}}) \right\} \tag{3.16}$$

with

$$\mathrm{SNR} = \frac{E}{\sigma^2} \tag{3.17}$$

Since the threshold τ is determined only by the false alarm constraint, it does not depend on the energy parameter. Therefore, the decision function that is optimal in the Neyman-Pearson sense, is also independent of the energy. Tests that are optimal for all values of signal parameters are called *uniformly most powerful* (UMP). The test in this section is UMP. For many detection problems however, no UMP test exists, [10].

3.3 Detection of a Known Vector in White Gaussian Noise

This section deals with the detection of a complex vector in white complex Gaussian noise. The vector is assumed to be known upto a scalar factor. In other words, the shape of the signal is known but the energy is unknown. Energy in this case is a deterministic parameter but its value is not available to the observer. A UMP test which does not depend on this parameter is derived.

In order to detach the energy from the shape of the signal, the shape is defined as a normalized vector. For a signal length of N, the shape of the signal $\mathbf{a} \in \mathbb{C}^N$ is a column vector with unit energy. Namely,

$$||\mathbf{a}||^2 = 1 \tag{3.18}$$

where $||\mathbf{a}|| = \sqrt{\mathbf{a}^*\mathbf{a}}$ is the 2-norm of the vector $\mathbf{a}$. $\mathbf{a}^*$ is the complex conjugate transpose of $\mathbf{a}$.

Now the signal $\mathbf{s} \in \mathbb{C}^N$ can be defined as

$$\mathbf{s} = \sqrt{E}\,\mathbf{a} \tag{3.19}$$

where $E \geq 0$ is the energy.

Note that calling E as the energy of the signal is valid since

$$||\mathbf{s}||^2 = \mathbf{a}^*\mathbf{a}E = ||\mathbf{a}||^2 E = E \tag{3.20}$$

Let the noise vector $\underset{\sim}{\mathbf{w}}$ be an N-dimensional circularly symmetric complex Gaussian vector with distribution $\mathcal{CN}(\mathbf{0}, \sigma^2\mathbf{I}_N)$ where $\mathbf{I}_N$ is the N-by-N identity matrix.

This problem can be solved by projecting the N-dimensional signal and the N-dimensional noise into a one dimensional space. This projection should keep the signal energy as much as possible while reducing most of the noise power. It turns out that the projected direction coincides with the direction of the signal itself. Filter implementation of this projection is called *matched filter* in literature.

Let

$$\boldsymbol{\phi}_0 = \frac{\mathbf{s}}{||\mathbf{s}||} \tag{3.21}$$

With $\boldsymbol{\phi}_0$ defined as above, let

$$\{\boldsymbol{\phi}_0, \boldsymbol{\phi}_1, \ldots, \boldsymbol{\phi}_{N-1}\} \tag{3.22}$$

be an orthonormal set in $\mathbb{C}^N$. One can find such a set by the Gram-Schmidt algorithm. Since the set is N dimensional, it forms a basis for $\mathbb{C}^N$.

Then for H_0,

$$\begin{aligned} \underset{\sim}{\mathbf{y}} &= \underset{\sim}{\mathbf{w}} \\ &= \sum_{n=0}^{N-1} \langle \underset{\sim}{\mathbf{w}}, \boldsymbol{\phi}_n \rangle \boldsymbol{\phi}_n \\ &= \langle \underset{\sim}{\mathbf{w}}, \boldsymbol{\phi}_0 \rangle \boldsymbol{\phi}_0 + \sum_{n=1}^{N-1} \langle \underset{\sim}{\mathbf{w}}, \boldsymbol{\phi}_n \rangle \boldsymbol{\phi}_n \end{aligned} \tag{3.23}$$

and for H_1,

$$\begin{aligned} \underset{\sim}{\mathbf{y}} &= \mathbf{s} + \underset{\sim}{\mathbf{w}} \\ &= \|\mathbf{s}\| \boldsymbol{\phi}_0 + \sum_{n=0}^{N-1} \langle \underset{\sim}{\mathbf{w}}, \boldsymbol{\phi}_n \rangle \boldsymbol{\phi}_n \\ &= \Big\{ \|\mathbf{s}\| + \langle \underset{\sim}{\mathbf{w}}, \boldsymbol{\phi}_0 \rangle \Big\} \boldsymbol{\phi}_0 + \sum_{n=1}^{N-1} \langle \underset{\sim}{\mathbf{w}}, \boldsymbol{\phi}_n \rangle \boldsymbol{\phi}_n \end{aligned} \tag{3.24}$$

Here, $\langle \mathbf{x}, \mathbf{y} \rangle = \mathbf{y}^* \mathbf{x}$ is the inner product of the vectors $\mathbf{x}$ and $\mathbf{y}$.

The term $\sum_{n=1}^{N-1} \langle \underset{\sim}{\mathbf{w}}, \boldsymbol{\phi}_n \rangle \boldsymbol{\phi}_n$ appears in both hypotheses, therefore it can be regarded as a nuisance parameter. It can be discarded from the observation. One can easily show

$$\sum_{n=1}^{N-1} \langle \underset{\sim}{\mathbf{w}}, \boldsymbol{\phi}_n \rangle \boldsymbol{\phi}_n = \sum_{n=1}^{N-1} \Big\langle \underset{\sim}{\mathbf{y}}, \boldsymbol{\phi}_n \Big\rangle \boldsymbol{\phi}_n \tag{3.25}$$

regardless of the hypothesis. Therefore we can discard all projections of the observation vector except onto ϕ_0. That is observe only

$$\underset{\sim}{y} = \Big\langle \underset{\sim}{\mathbf{y}}, \boldsymbol{\phi}_0 \Big\rangle = \left\langle \underset{\sim}{\mathbf{y}}, \frac{\mathbf{s}}{\|\mathbf{s}\|} \right\rangle = \mathbf{a}^* \underset{\sim}{\mathbf{y}} \tag{3.26}$$

With the above discussion detection problem is reduced to the following one dimensional problem.

$$\begin{aligned} H_0 &: \underset{\sim}{y} = \underset{\sim}{w} \\ H_1 &: \underset{\sim}{y} = \|\mathbf{s}\| + \underset{\sim}{w} \end{aligned} \tag{3.27}$$

where $\underset{\sim}{w} = \left\langle \underset{\sim}{\mathbf{w}}, \frac{\mathbf{s}}{\|\mathbf{s}\|} \right\rangle$.

But again, $\mathrm{Im}\{\underset{\sim}{y}\}$, which is equal to $\mathrm{Im}\{\underset{\sim}{w}\}$, is the same for both hypotheses since $\|\mathbf{s}\|$ is always real. It can be discarded as well. Only the real part is observed. The problem is moreover reduced to

$$\begin{aligned} H_0 &: \underset{\sim}{y}' = \mathrm{Re}\{\underset{\sim}{w}\} \\ H_1 &: \underset{\sim}{y}' = \|\mathbf{s}\| + \mathrm{Re}\{\underset{\sim}{w}\} \end{aligned} \tag{3.28}$$

where $\underset{\sim}{y}' = \mathrm{Re}\left\{\underset{\sim}{y}\right\} = \mathrm{Re}\left\{\mathbf{a}^* \underset{\sim}{\mathbf{y}}\right\}$.

Since $\mathrm{Re}\{\underset{\sim}{w}\}$ is the real part of a linear combination of Gaussian random variables it is also Gaussian.

For H_0,

$$\begin{aligned} \mathrm{E}\{\underset{\sim}{y}'\} &= \mathrm{E}\left\{\mathrm{Re}\{\underset{\sim}{w}\}\right\} \\ &= \mathrm{Re}\left\{\mathrm{E}\{\boldsymbol{\phi}_0^* \underset{\sim}{\mathbf{w}}\}\right\} \\ &= \mathrm{Re}\left\{\boldsymbol{\phi}_0^* \, \mathrm{E}\{\underset{\sim}{\mathbf{w}}\}\right\} \\ &= 0 \end{aligned} \tag{3.29}$$

$$\begin{aligned} \mathrm{var}\{\underset{\sim}{y}'\} &= \mathrm{var}\left\{\mathrm{Re}\{\underset{\sim}{w}\}\right\} \\ &= \mathrm{var}\left\{\frac{\boldsymbol{\phi}_0^* \underset{\sim}{\mathbf{w}} + \underset{\sim}{\mathbf{w}}^* \boldsymbol{\phi}_0}{2}\right\} \\ &= \frac{\|\boldsymbol{\phi}_0\|^2 \, \mathrm{var}\{\underset{\sim}{\mathbf{w}}\} + \|\boldsymbol{\phi}_0\|^2 \, \mathrm{var}\{\underset{\sim}{\mathbf{w}}^*\}}{4} \\ &= \frac{\sigma^2}{2} \end{aligned} \tag{3.30}$$

For H_1,

$$\begin{aligned} \mathrm{E}\{\underset{\sim}{y}'\} &= \mathrm{E}\left\{\|s\| + \mathrm{Re}\{\underset{\sim}{w}\}\right\} \\ &= \|s\| + \mathrm{E}\left\{\mathrm{Re}\{\underset{\sim}{w}\}\right\} \\ &= \|s\| \end{aligned} \tag{3.31}$$

$$\mathrm{var}\{\underset{\sim}{y}'\} = \frac{\sigma^2}{2} \tag{3.32}$$

The distributions for both of the hypotheses are now known. The reduced problem is exactly the same as the one solved in section 3.2 with the same energy parameter. The variance however must be replaced by the half of it. Note that the reduced problem does not depend on the shape of the signal but depends on its energy. This means, whatever shape is used for transmission, if the observer knows the normalized shape, the detection performance stays the same.

Since the modified detection problem in this section is the same with the one in section 3.2 with variance replaced by the half of it, we can find the relation between the threshold and the false alarm probability by replacing σ by $\sigma/\sqrt{2}$ in equation (3.15).

Summary The detection problem in this section can be summarized as below.

$$\begin{aligned} H_0 &: \underset{\sim}{\mathbf{y}} \sim \mathcal{CN}\left(\mathbf{0}, \sigma^2 \mathbf{I}_N\right) \\ H_1 &: \underset{\sim}{\mathbf{y}} \sim \mathcal{CN}\left(\sqrt{E}\mathbf{a}, \sigma^2 \mathbf{I}_N\right) \end{aligned} \tag{3.33}$$

The decision function that is optimal in the Neyman-Pearson sense:

$$\eth_{\mathrm{NP}}(\mathbf{y}) = \begin{cases} 1 & \text{if } \mathrm{Re}\{\mathbf{a}^* \mathbf{y}\} > \tau \\ 0 & \text{otherwise} \end{cases} \tag{3.34}$$

where

$$\tau = \frac{\sigma}{\sqrt{2}} \mathrm{Q}^{-1}(P_{\mathrm{FA}}) \tag{3.35}$$

The ROC curve belonging to $\eth_{\mathrm{NP}}$ is given as

$$P_{\mathrm{D}} = 1 - \mathrm{Q}\left\{\sqrt{2\,\mathrm{SNR}} - \mathrm{Q}^{-1}(P_{\mathrm{FA}})\right\} \tag{3.36}$$

where

$$\mathrm{SNR} = \frac{E}{\sigma^2} \tag{3.37}$$

It can also be preferred to implement this detector without normalizing the signal. In this case however, threshold calculation would depend on the signal energy which may not be known beforehand.

3.4 Detection of a Known Vector in Colored Gaussian Noise

This section deals with the detection of a complex vector in colored complex Gaussian noise. The signal is defined as in section 3.3 with E as the energy and $\mathbf{a}$ as the normalized shape vector.

Let the noise vector $\underset{\sim}{\mathbf{y}}$ be an N-dimensional circularly symmetric complex Gaussian vector with distribution $\mathcal{CN}(\mathbf{0}, \mathbf{\Gamma})$ where $\mathbf{\Gamma}$ is the N-by-N covariance matrix.

This problem can be solved in two steps. The first is to whiten the noise by applying a whitening transformation to the obsevation vector. Then the resultant transformed vector can be projected on the signal as discussed in section 3.3.

Let the sets $\{\lambda_0, \lambda_1, \ldots, \lambda_{N-1}\}$ and $\{\boldsymbol{\phi}_0, \boldsymbol{\phi}_1, \ldots, \boldsymbol{\phi}_{N-1}\}$ be the collections of eigenvalues and normalized eigenvectors of $\mathbf{\Gamma}$ respectively. In other words, they satisfy

$$\|\boldsymbol{\phi}_i\| = 1 \quad \text{and} \quad \mathbf{\Gamma}\boldsymbol{\phi}_i = \lambda_i \boldsymbol{\phi}_i \quad \text{for all } i = 0, 1, \ldots, N-1 \tag{3.38}$$

We need to whiten the noise. Let the transformation matrix $\mathbf{T}$ be defined as

$$\mathbf{T} = \mathbf{\Lambda}^{-1/2}\mathbf{\Phi}^* \tag{3.39}$$

where $\mathbf{\Lambda}$ is an N-by-N diagonal matrix with i^{th} diagonal element equal to λ_i and $\mathbf{\Phi}$ is an N-by-N matrix with i^{th} column equal to $\boldsymbol{\phi}_i$.

$\mathbf{T}$ is a whitening transformation matrix since if $\underset{\sim}{\mathbf{w}} = \mathbf{T}\underset{\sim}{\mathbf{y}}$,

$$\begin{aligned} \mathrm{E}\{\underset{\sim}{\mathbf{w}}\} &= \mathrm{E}\{\mathbf{T}\underset{\sim}{\mathbf{y}}\} \\ &= \mathrm{E}\left\{\mathbf{\Lambda}^{-1/2}\mathbf{\Phi}^*\underset{\sim}{\mathbf{y}}\right\} \\ &= \mathbf{\Lambda}^{-1/2}\mathbf{\Phi}^*\,\mathrm{E}\{\underset{\sim}{\mathbf{y}}\} \\ &= 0 \end{aligned} \tag{3.40}$$

$$
\begin{aligned}
\text{var}\{\underset{\sim}{\mathbf{w}}\} &= \text{E}\{\mathbf{T}\underset{\sim}{\mathbf{y}}\underset{\sim}{\mathbf{y}}^*\mathbf{T}^*\} \\
&= \text{E}\{\mathbf{\Lambda}^{-1/2}\mathbf{\Phi}^*\underset{\sim}{\mathbf{y}}\underset{\sim}{\mathbf{y}}^*\mathbf{\Phi}\mathbf{\Lambda}^{-1/2}\} \\
&= \mathbf{\Lambda}^{-1/2}\mathbf{\Phi}^*\,\text{E}\{\underset{\sim}{\mathbf{y}}\underset{\sim}{\mathbf{y}}^*\}\mathbf{\Phi}\mathbf{\Lambda}^{-1/2} \\
&= \mathbf{\Lambda}^{-1/2}\mathbf{\Phi}^*\mathbf{\Gamma}\mathbf{\Phi}\mathbf{\Lambda}^{-1/2} \\
&= \mathbf{\Lambda}^{-1/2}\mathbf{\Phi}^*\mathbf{\Phi}\mathbf{\Lambda}\mathbf{\Phi}^*\mathbf{\Phi}\mathbf{\Lambda}^{-1/2} \\
&= \mathbf{\Lambda}^{-1/2}\mathbf{\Lambda}\mathbf{\Lambda}^{-1/2} \\
&= \mathbf{I}_N
\end{aligned} \tag{3.41}
$$

If we transform the observations by $\mathbf{T}$, the problem becomes

$$
\begin{aligned}
H_0 &: \underset{\sim}{\mathbf{y}}' = \underset{\sim}{\mathbf{w}} \\
H_1 &: \underset{\sim}{\mathbf{y}}' = \mathbf{T}\mathbf{s} + \underset{\sim}{\mathbf{w}}
\end{aligned} \tag{3.42}
$$

where $\underset{\sim}{\mathbf{y}}' = \mathbf{T}\underset{\sim}{\mathbf{y}}$ and $\underset{\sim}{\mathbf{w}} \sim \mathcal{CN}(\mathbf{0}, \mathbf{I}_N)$.

But this is the exact problem introduced in section 3.3 with unity variance. After the transformation, the resultant normalized shape becomes

$$
\mathbf{a}' = \frac{\mathbf{T}\mathbf{a}}{\|\mathbf{T}\mathbf{a}\|} = \frac{\mathbf{\Lambda}^{-1/2}\mathbf{\Phi}^*\mathbf{a}}{\|\mathbf{\Lambda}^{-1/2}\mathbf{\Phi}^*\mathbf{a}\|} \tag{3.43}
$$

and the observation vector

$$
\mathbf{y}' = \mathbf{T}\mathbf{y} = \mathbf{\Lambda}^{-1/2}\mathbf{\Phi}^*\mathbf{y} \tag{3.44}
$$

The tested variable in equation (3.34) then becomes

$$
\text{Re}\{\mathbf{a}'^*\mathbf{y}'\} = \text{Re}\left\{\frac{\mathbf{a}^*\mathbf{\Phi}\mathbf{\Lambda}^{-1}\mathbf{\Phi}^*}{\|\mathbf{\Lambda}^{-1/2}\mathbf{\Phi}^*\mathbf{a}\|}\mathbf{y}\right\} \tag{3.45}
$$

Summary The detection problem in this section can be summarized as below.

$$
\begin{aligned}
H_0 &: \underset{\sim}{\mathbf{y}} \sim \mathcal{CN}(\mathbf{0}, \mathbf{\Gamma}) \\
H_1 &: \underset{\sim}{\mathbf{y}} \sim \mathcal{CN}\left(\sqrt{E}\mathbf{a}, \mathbf{\Gamma}\right)
\end{aligned} \tag{3.46}
$$

The decision function that is optimal in the Neyman-Pearson sense:

$$
\eth_{\text{NP}}(\mathbf{y}) = \begin{cases} 1 & \text{if } \text{Re}\left\{\dfrac{\mathbf{a}^*\mathbf{\Phi}\mathbf{\Lambda}^{-1}\mathbf{\Phi}^*}{\|\mathbf{\Lambda}^{-1/2}\mathbf{\Phi}^*\mathbf{a}\|}\mathbf{y}\right\} > \tau \\ 0 & \text{otherwise} \end{cases} \tag{3.47}
$$

where

$$\tau = \frac{1}{\sqrt{2}} \mathrm{Q}^{-1}(P_{\mathrm{FA}}) \tag{3.48}$$

The ROC curve belonging to $\eth_{\mathrm{NP}}$ is given as

$$P_{\mathrm{D}} = 1 - \mathrm{Q}\left\{ \sqrt{2\,\mathrm{SNR}} - \mathrm{Q}^{-1}(P_{\mathrm{FA}}) \right\} \tag{3.49}$$

where

$$\mathrm{SNR} = \|\mathbf{\Lambda}^{-1/2}\mathbf{\Phi}^{*}\mathbf{a}\|^2 E \tag{3.50}$$

To the contrary of the case in section 3.3, the probability of detection in this case depends on the signal shape.

Let $\lambda_{\min} = \min\{\lambda_0, \lambda_1, \ldots, \lambda_{N-1}\}$. If the shape of the signal is defined as below

$$\mathbf{a} = \sum_{\{i:\lambda_i = \lambda_{\min}\}} c_i\, \boldsymbol{\delta}_i \tag{3.51}$$

for some complex constants c_i such that $\sum_{\{i:\lambda_i=\lambda_{\min}\}} |c_i|^2 = 1$, then signal to noise ratio will be maximized. In the above equation, $\boldsymbol{\delta}_i$ is a column vector of all zeros except the i^{th} element which is one. This means that if signal is nonzero only at those samples which noise variance is minimum, then SNR is maximum.

Some examples of ROC curves are plotted for different SNR values in Figure 3.1. In order to read low P_{FA} region, x-axis may be preferred to be log-scaled. Figure 3.2 plots the same curves in log scale.

When the covariance matrix $\mathbf{\Gamma}$ is a diagonal matrix with all the diagonal elements being equal, the detection problem in this section becomes exactly the same as the problem in section 3.3. Since the SNR values in both cases would then result in the same values, the ROC curve plots given in this section also applies to the section 3.3.

3.5 Detection of a Signal with Random Phase

In this section, a random phase will be added to signal definition. The phase is modeled as a uniformly distributed random variable. This parameter however is integrated out in the Bayesian formulation leaving a test independent of its realization.

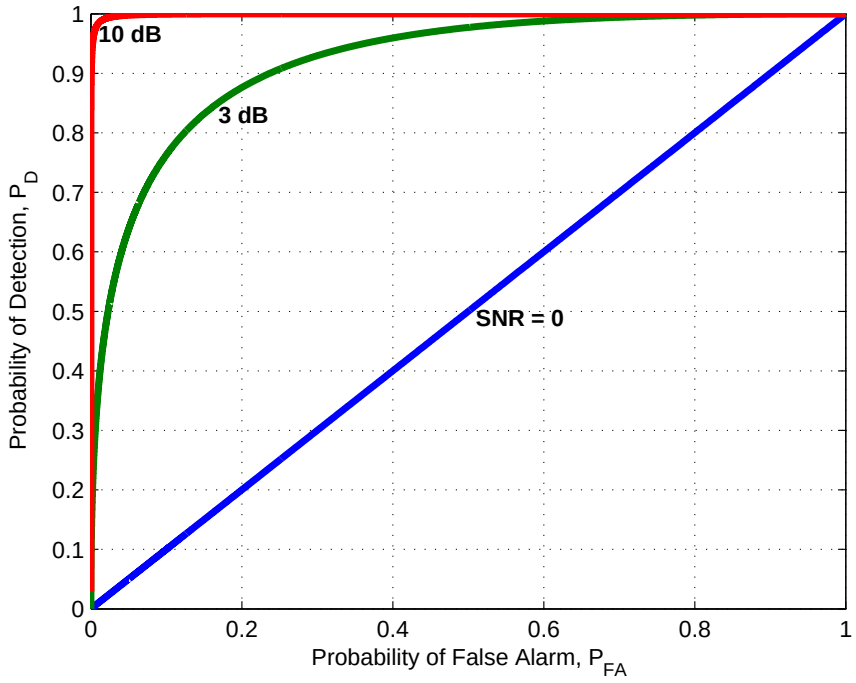

Figure 3.1: Performance of the decision function given in (3.47) for several SNR values.

Let the signal be defined as

$$\underset{\sim}{\mathbf{s}} = \sqrt{E}\,\mathbf{a}\,e^{j\underset{\sim}{\theta}} \tag{3.52}$$

where

- $E \geq 0$ is the energy of the signal.
- $\mathbf{a} \in \mathbb{C}^N$ is a column vector of the shape of the signal satisfying $\|\mathbf{a}\|^2 = 1$.
- $\underset{\sim}{\theta}$ which is uniformly distributed in the interval $[0, 2\pi)$ is the phase of the signal.

Let the noise vector $\underset{\sim}{\mathbf{w}}$ be an N-dimensional circular symmetric complex Gaussian vector with distribution $\mathcal{CN}\left(\mathbf{0}, \sigma^2\mathbf{I}_N\right)$.

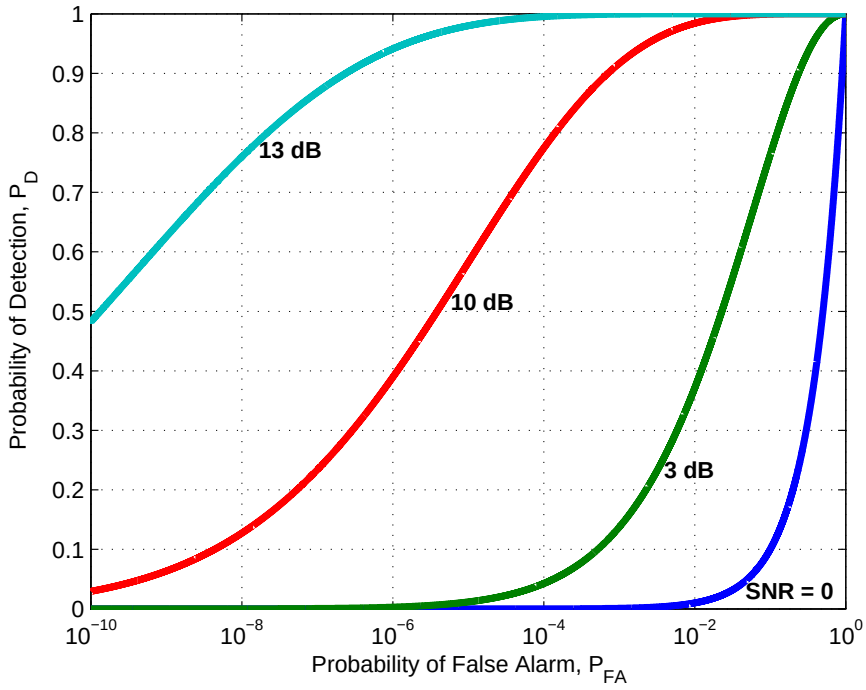

Figure 3.2: Performance of the decision function given in (3.47) for several SNR values. The P_{FA} axis is in log-scale.

We can find $p_{\underset{\sim}{\mathbf{y}}}(\mathbf{y} \mid H_1)$ by conditioning on the parameter $\underset{\sim}{\theta}$.

$$
\begin{aligned}
p_{\underset{\sim}{\mathbf{y}}}(\mathbf{y} \mid H_1) &= \int_0^{2\pi} p_{\underset{\sim}{\mathbf{y}}}(\mathbf{y} \mid \underset{\sim}{\theta} = \theta, H_1) p_{\underset{\sim}{\theta}}(\theta)\, \mathrm{d}\theta \\
&= \int_0^{2\pi} \frac{1}{\pi^N \sigma^{2N}} \exp\left\{ -\frac{1}{\sigma^2} \left(\mathbf{y} - \sqrt{E}\mathbf{a}e^{j\theta}\right)^* \left(\mathbf{y} - \sqrt{E}\mathbf{a}e^{j\theta}\right) \right\} \frac{1}{2\pi}\, \mathrm{d}\theta \\
&= \frac{1}{\pi^N \sigma^{2N}} \frac{1}{2\pi} \int_0^{2\pi} \exp\left\{ -\frac{1}{\sigma^2} \left(\mathbf{y}^*\mathbf{y} - \sqrt{E}\mathbf{y}^*\mathbf{a}e^{j\theta} - \sqrt{E}\mathbf{a}^*\mathbf{y}e^{-j\theta} + E\right) \right\} \mathrm{d}\theta \\
&= \frac{1}{\pi^N \sigma^{2N}} \exp\left\{ -\frac{\mathbf{y}^*\mathbf{y} + E}{\sigma^2} \right\} \frac{1}{2\pi} \int_0^{2\pi} \exp\left\{ \frac{\sqrt{E}}{\sigma^2} \left(\mathbf{y}^*\mathbf{a}e^{j\theta} + \mathbf{a}^*\mathbf{y}e^{-j\theta}\right) \right\} \mathrm{d}\theta \\
&= \frac{1}{\pi^N \sigma^{2N}} \exp\left\{ -\frac{\mathbf{y}^*\mathbf{y} + E}{\sigma^2} \right\} \frac{1}{2\pi} \int_0^{2\pi} \exp\left\{ \frac{\sqrt{E}}{\sigma^2} \left(|\mathbf{a}^*\mathbf{y}|e^{j(\theta-\phi)} + |\mathbf{a}^*\mathbf{y}|e^{-j(\theta-\phi)}\right) \right\} \mathrm{d}\theta \\
&= \frac{1}{\pi^N \sigma^{2N}} \exp\left\{ -\frac{\mathbf{y}^*\mathbf{y} + E}{\sigma^2} \right\} \frac{1}{2\pi} \int_0^{2\pi} \exp\left\{ \frac{2\sqrt{E}|\mathbf{a}^*\mathbf{y}|}{\sigma^2} \cos(\theta - \phi) \right\} \mathrm{d}\theta \\
&= \frac{1}{\pi^N \sigma^{2N}} \exp\left\{ -\frac{\mathbf{y}^*\mathbf{y} + E}{\sigma^2} \right\} \mathcal{I}_0\left(\frac{2\sqrt{E}|\mathbf{a}^*\mathbf{y}|}{\sigma^2} \right)
\end{aligned}
\tag{3.53}
$$

where

$$\mathcal{I}_0(x) = \frac{1}{2\pi}\int_0^{2\pi} e^{x\cos(\theta-\phi)}\,\mathrm{d}\theta \tag{3.54}$$

is the modified Bessel function of the first kind. Also in the above equations ϕ is equal to the phase of the complex number $\mathbf{a}^*\mathbf{y}$.

Now, the likelihood ratio can be written as:

$$\begin{aligned}
\mathrm{L}(\mathbf{y}) &= \frac{p_{\underset{\sim}{\mathbf{y}}}(\mathbf{y} \mid H_1)}{p_{\underset{\sim}{\mathbf{y}}}(\mathbf{y} \mid H_0)} \\
&= \frac{\frac{1}{\pi^N\sigma^{2N}}\exp\left\{-\frac{(\mathbf{y}^*\mathbf{y}+E)}{\sigma^2}\right\}\mathcal{I}_0\left(\frac{2\sqrt{E}|\mathbf{a}^*\mathbf{y}|}{\sigma^2}\right)}{\frac{1}{\pi^N\sigma^{2N}}\exp\left\{-\frac{\mathbf{y}^*\mathbf{y}}{\sigma^2}\right\}} \\
&= \exp\left\{-\frac{E}{\sigma^2}\right\}\mathcal{I}_0\left(\frac{2\sqrt{E}|\mathbf{a}^*\mathbf{y}|}{\sigma^2}\right)
\end{aligned} \tag{3.55}$$

Decision test using log-likelihood ratio is

$$\begin{aligned}
\ln \mathrm{L}(\mathbf{y}) &= -\frac{E}{\sigma^2} + \ln\left\{\mathcal{I}_0\left(\frac{2\sqrt{E}|\mathbf{a}^*\mathbf{y}|}{\sigma^2}\right)\right\} > \gamma \\
&\Rightarrow \ln\left\{\mathcal{I}_0\left(\frac{2\sqrt{E}|\mathbf{a}^*\mathbf{y}|}{\sigma^2}\right)\right\} > \gamma + \frac{E}{\sigma^2} \\
&\Rightarrow \mathcal{I}_0\left(\frac{2\sqrt{E}|\mathbf{a}^*\mathbf{y}|}{\sigma^2}\right) > \exp\left(\gamma + \frac{E}{\sigma^2}\right)
\end{aligned} \tag{3.56}$$

$\mathcal{I}_0$ is a monotonically increasing function. Therefore we can rewrite the relation in (3.56) as

$$\begin{aligned}
\frac{2\sqrt{E}|\mathbf{a}^*\mathbf{y}|}{\sigma^2} &> \mathcal{I}_0^{-1}\left\{\exp\left(\gamma + \frac{E}{\sigma^2}\right)\right\} \\
\Rightarrow |\mathbf{a}^*\mathbf{y}| &> \tau
\end{aligned} \tag{3.57}$$

where $\tau = \frac{\sigma^2}{2\sqrt{E}}\mathcal{I}_0^{-1}\left\{\exp\left(\gamma + \frac{E}{\sigma^2}\right)\right\}$ is a threshold to be found from false alarm constraint.

The distribution for $\mathbf{a}^*\mathbf{y}$ is Gaussian, therefore the distribution for the random variable $\underset{\sim}{z} = |\mathbf{a}^*\mathbf{y}|$ is the Rice distribution.

For H_0

$$\mathrm{E}\{\mathbf{a}^*\mathbf{y}\} = 0 \tag{3.58}$$

$$\mathrm{var}\{\mathbf{a}^*\mathbf{y}\} = \|\mathbf{a}\|^2\,\mathrm{var}\{y\} = \sigma^2 \tag{3.59}$$

$$p_{\underset{\sim}{z}}(z \mid H_0) = \frac{2z}{\sigma^2}\exp\left(\frac{-z^2}{\sigma^2}\right) \tag{3.60}$$

and for H_1

$$\mathrm{E}\{\mathbf{a}^*\mathbf{y}\} = \sqrt{E}e^{j\theta} \tag{3.61}$$

$$\mathrm{var}\{\mathbf{a}^*\mathbf{y}\} = \sigma^2 \tag{3.62}$$

$$p_{\underset{\sim}{z}}(z \mid H_1) = \frac{2z}{\sigma^2}\exp\left(-\frac{z^2+E}{\sigma^2}\right)\mathcal{I}_0\left(\frac{2z\sqrt{E}}{\sigma^2}\right) \tag{3.63}$$

The false alarm and detection probabilities can be calculated as

$$\begin{aligned} P_{\mathrm{FA}}(\tau) &= \int_{\tau}^{\infty}\frac{2z}{\sigma^2}\exp\left(\frac{-z^2}{\sigma^2}\right)\mathrm{d}z \\ &= \exp\left(\frac{-\tau^2}{\sigma^2}\right) \end{aligned} \tag{3.64}$$

$$\begin{aligned} P_{\mathrm{D}}(\tau) &= \int_{\tau}^{\infty}\frac{2z}{\sigma^2}\exp\left(-\frac{z^2+E}{\sigma^2}\right)\mathcal{I}_0\left(\frac{2z\sqrt{E}}{\sigma^2}\right)\mathrm{d}z \\ &= \mathrm{Q}_1\left(\frac{\sqrt{2E}}{\sigma}, \frac{\sqrt{2\tau^2}}{\sigma}\right) \end{aligned} \tag{3.65}$$

where

$$\mathrm{Q}_1(a,b) = \int_{b}^{\infty} x\exp\left(-\frac{x^2+a^2}{2}\right)\mathcal{I}_0(ax)\,\mathrm{d}x \tag{3.66}$$

is the first order Marcum Q function. [37]

Summary The detection problem in this section can be summarized as below.

$$\begin{aligned} &H_0 : \underset{\sim}{\mathbf{y}} \sim \mathcal{CN}\left(\mathbf{0}, \sigma^2\mathbf{I}_N\right) \\ &H_1 : \underset{\sim}{\mathbf{y}} \sim \mathcal{CN}\left(\sqrt{E}\mathbf{a}e^{j\theta}, \sigma^2\mathbf{I}_N\right) \quad \text{given } \underset{\sim}{\theta} = \theta \end{aligned} \tag{3.67}$$

The decision function that is optimal in the Neyman-Pearson sense:

$$\vartheta_{\mathrm{NP}}(\mathbf{y}) = \begin{cases} 1 & \text{if } |\mathbf{a}^*\mathbf{y}| > \tau \\ 0 & \text{otherwise} \end{cases} \tag{3.68}$$

where

$$\tau = \sqrt{-\sigma^2 \ln P_{\mathrm{FA}}} \tag{3.69}$$

The ROC curve belonging to $\eth_{\text{NP}}$ is given as

$$P_{\text{D}} = \text{Q}_1\left(\sqrt{2\,\text{SNR}},\ \sqrt{-2\ln P_{\text{FA}}}\right) \tag{3.70}$$

where

$$\text{SNR} = \frac{E}{\sigma^2} \tag{3.71}$$

Figure 3.3 plots the ROC curves belonging to the decision function. If this figure is compared with Figure 3.2 it can be seen that for random phase case, the probability of detection is lower. This is expected since in this case, less is known about the signal to be detected. Higher SNR is needed for the same detection performance.

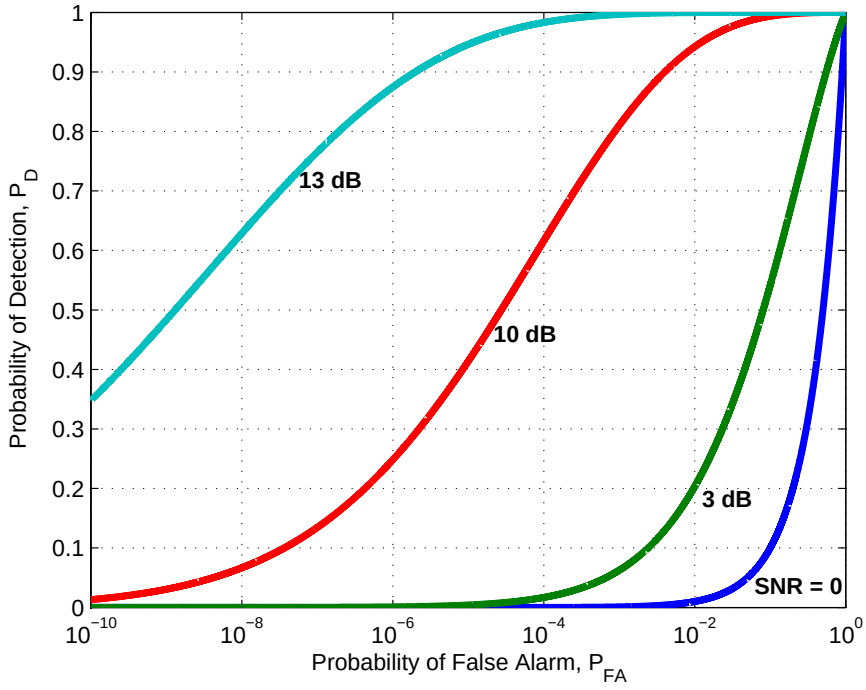

Figure 3.3: Performance of the decision function given in (3.70) for several SNR values.

3.6 Detection of a Signal with Random Phase and Frequency

Let $\mathbf{a} \in \mathbb{C}^N$ be the normalized envelope of the signal. Let the signal be defined as

$$s_n = \sqrt{E}\ a_n\ e^{j(\omega n + \theta)} \quad \text{for } n = 0, 1, \ldots, N-1. \tag{3.72}$$

where

- $E \geq 0$ is the energy of the signal.
- a_n is the n-th element of $\mathbf{a}$.
- $\underset{\sim}{\omega}$ defined in the interval $[0, 2\pi)$ with probability density function $p_{\underset{\sim}{\omega}}(.)$ is the radial frequency of the signal.
- $\underset{\sim}{\theta}$ which is uniformly distributed in the interval $[0, 2\pi)$ is the phase of the signal.

The frequency and phase are independent.

In vector notation, the signal can be represented as

$$\underset{\sim}{\mathbf{s}} = \sqrt{E}\, \mathbf{A}\, \boldsymbol{\xi}(\underset{\sim}{\omega})\, e^{j\underset{\sim}{\theta}} \tag{3.73}$$

where

- $\mathbf{A}(\underset{\sim}{N})$ is an N-by-N diagonal matrix with n-th diagonal element being equal to a_n.
- $\boldsymbol{\xi}(\underset{\sim}{\omega})$ is a column vector. Its n-th element is defined as

$$\xi_n(\underset{\sim}{\omega}) = e^{j\underset{\sim}{\omega} n} \quad \text{for } n = 0, 1, \ldots, N-1 \tag{3.74}$$

Let the noise vector $\underset{\sim}{\mathbf{w}}$ be an N-dimensional circular symmetric complex Gaussian vector with distribution $\mathcal{CN}\left(\mathbf{0}, \sigma^2 \mathbf{I}_N\right)$.

By adapting equation (3.53) to the definition of the signal in this section

$$p_{\underset{\sim}{\mathbf{y}}}(\mathbf{y} \mid \underset{\sim}{\omega} = \omega, H_1) = \frac{1}{\pi^N \sigma^{2N}} \exp\left\{-\frac{(\mathbf{y}^*\mathbf{y} + E)}{\sigma^2}\right\} \mathcal{I}_0\left(\frac{2\sqrt{E}}{\sigma^2}\left|\boldsymbol{\xi}^*(\omega)\mathbf{A}^*\mathbf{y}\right|\right) \tag{3.75}$$

If $p_{\underset{\sim}{\mathbf{y}}}(\mathbf{y} \mid H_1)$ is calculated by conditioning on $\underset{\sim}{\omega}$

$$\begin{aligned} p_{\underset{\sim}{\mathbf{y}}}(\mathbf{y} \mid H_1) &= \int_0^{2\pi} p_{\underset{\sim}{\mathbf{y}}}(\mathbf{y} \mid \underset{\sim}{\omega} = \omega, H_1) p_{\underset{\sim}{\omega}}(\omega)\, \mathrm{d}\omega \\ &= \frac{1}{\pi^N \sigma^{2N}} \exp\left\{-\frac{(\mathbf{y}^*\mathbf{y} + E)}{\sigma^2}\right\} \int_0^{2\pi} \mathcal{I}_0\left(\frac{2\sqrt{E}}{\sigma^2}\left|\boldsymbol{\xi}^*(\omega)\mathbf{A}^*\mathbf{y}\right|\right) p_{\underset{\sim}{\omega}}(\omega)\, \mathrm{d}\omega \end{aligned} \tag{3.76}$$

The likelihood ratio is equal to

$$\mathrm{L}(\mathbf{y}) = \exp\left\{-\frac{E}{\sigma^2}\right\} \int_0^{2\pi} \mathcal{I}_0\left(\frac{2\sqrt{E}}{\sigma^2}\left|\boldsymbol{\xi}^*(\omega)\mathbf{A}^*\mathbf{y}\right|\right) p_{\underset{\sim}{\omega}}(\omega)\, \mathrm{d}\omega \tag{3.77}$$

The decision test may depend on thresholding the likelihood in (3.77). The integration however is difficult to compute and the resultant test may be dependent on the value of energy which is not desired.

In order to overcome these difficulties, another approach, the *generalized likelihood ratio test* (GLRT) will be used. In this approach, estimates of the unknown variables are used when finding the likelihood ratio.

If MAP estimate is used for the random variable $\underset{\sim}{\omega}$

$$\begin{aligned}\hat{\omega} &= \arg\max_{\omega\in[0,2\pi)} \left\{ p_{\underset{\sim}{\mathbf{y}}}(\mathbf{y} \mid \underset{\sim}{\omega} = \omega, H_1) p_{\underset{\sim}{\omega}}(\omega) \right\} \\ &= \arg\max_{\omega\in[0,2\pi)} \left\{ \frac{1}{\pi^N \sigma^{2N}} \exp\left\{ -\frac{(\mathbf{y}^*\mathbf{y} + E)}{\sigma^2} \right\} \mathcal{I}_0\left(\frac{2\sqrt{E}}{\sigma^2} \left| \boldsymbol{\xi}^*(\omega)\mathbf{A}^*\mathbf{y} \right| \right) p_{\underset{\sim}{\omega}}(\omega) \right\} \\ &= \arg\max_{\omega\in[0,2\pi)} \left\{ \mathcal{I}_0\left(\frac{2\sqrt{E}}{\sigma^2} \left| \boldsymbol{\xi}^*(\omega)\mathbf{A}^*\mathbf{y} \right| \right) p_{\underset{\sim}{\omega}}(\omega) \right\} \end{aligned} \tag{3.78}$$

Let $\mathcal{W}$ be a subset of $[0, 2\pi)$. If the probability density of $\underset{\sim}{\omega}$ is uniform in $\mathcal{W}$ and zero otherwise, then,

$$\hat{\omega} = \arg\max_{\omega\in\mathcal{W}} \left\{ \mathcal{I}_0\left(\frac{2\sqrt{E}}{\sigma^2} \left| \boldsymbol{\xi}^*(\omega)\mathbf{A}^*\mathbf{y} \right| \right) \right\} \tag{3.79}$$

Using the monotonically increasing property of $\mathcal{I}_0$,

$$\begin{aligned}\hat{\omega} &= \arg\max_{\omega\in\mathcal{W}} \left\{ \frac{2\sqrt{E}}{\sigma^2} \left| \boldsymbol{\xi}^*(\omega)\mathbf{A}^*\mathbf{y} \right| \right\} \\ &= \arg\max_{\omega\in\mathcal{W}} \left| \boldsymbol{\xi}^*(\omega)\mathbf{A}^*\mathbf{y} \right| \end{aligned} \tag{3.80}$$

The test using generalized likelihood ratio is written as:

$$\begin{aligned} \mathrm{L_G}(\mathbf{y} \mid \underset{\sim}{\omega} = \hat{\omega}) = \frac{p_{\underset{\sim}{\mathbf{y}}}(\mathbf{y} \mid \underset{\sim}{\omega} = \hat{\omega}, H_1)}{p_{\underset{\sim}{\mathbf{y}}}(\mathbf{y} \mid H_0)} &> \lambda \\ \Rightarrow \exp\left\{ -\frac{E}{\sigma^2} \right\} \mathcal{I}_0\left(\frac{2\sqrt{E}}{\sigma^2} \left| \boldsymbol{\xi}^*(\hat{\omega})\mathbf{A}^*\mathbf{y} \right| \right) &> \lambda \\ \Rightarrow \mathcal{I}_0\left(\frac{2\sqrt{E}}{\sigma^2} \left| \boldsymbol{\xi}^*(\hat{\omega})\mathbf{A}^*\mathbf{y} \right| \right) &> \lambda \exp\left\{ \frac{E}{\sigma^2} \right\} \\ \Rightarrow \frac{2\sqrt{E}}{\sigma^2} \left| \boldsymbol{\xi}^*(\hat{\omega})\mathbf{A}^*\mathbf{y} \right| &> \mathcal{I}_0^{-1}\left(\lambda \exp\left\{ \frac{E}{\sigma^2} \right\} \right) \\ \Rightarrow \left| \boldsymbol{\xi}^*(\hat{\omega})\mathbf{A}^*\mathbf{y} \right| &> \frac{\sigma^2}{2\sqrt{E}} \mathcal{I}_0^{-1}\left(\lambda \exp\left\{ \frac{E}{\sigma^2} \right\} \right) \\ \Rightarrow \max_{\omega\in\mathcal{W}} \left| \boldsymbol{\xi}^*(\omega)\mathbf{A}^*\mathbf{y} \right| &> \tau \end{aligned} \tag{3.81}$$

where $\tau = \frac{\sigma^2}{2\sqrt{E}} \mathcal{I}_0^{-1}\left(\lambda \exp\left\{\frac{E}{\sigma^2}\right\}\right)$ is a threshold to be found from false alarm constraint.

In order to perform (3.81) numerically, $\mathcal{W}$ must be sampled. Let N' be a scalar such that $N' \geq N$. Let $\mathcal{K}_{N'} = \{k : k = 0, 1, \ldots, N'-1,\ 2\pi k/N' \in \mathcal{W}\}$. If $\mathcal{W}$ is uniformly sampled at N points, that is $\omega_k = \frac{2\pi k}{N'}$, then the test becomes

$$\max_{k \in \mathcal{K}_{N'}} \left| \boldsymbol{\xi}^*\left(\frac{2\pi k}{N'}\right) \mathbf{A}^* \mathbf{y} \right| > \tau \tag{3.82}$$

Note that "$\boldsymbol{\xi}^*\left(\frac{2\pi k}{N'}\right)\mathbf{A}^*\mathbf{y}$" is the value of the k-th bin of the N'-point discrete Fourier transform (DFT) of the vector $\mathbf{A}^*\mathbf{y}$. If N' is not equal to N, zero padding is applied first to the end of the signal. Also note that that (3.82) is an approximation to (3.81) and it gets closer to the generalized likelihood ratio test as N' is increased.

At this point, for simplicity of calculations, the envelope of the signal can be chosen as rectangular. Namely,

$$a_n = \frac{1}{\sqrt{N}} \quad \text{for } n = 0, 1, \ldots, N-1 \tag{3.83}$$

In this case, the detector can be modified as not to include the additional multiplier $\frac{1}{\sqrt{N}}$. Namely the modified test becomes

$$\max_{k \in \mathcal{K}_{N'}} \left| \boldsymbol{\xi}^*\left(\frac{2\pi k}{N'}\right) \mathbf{y} \right| > \tau' \tag{3.84}$$

where $\tau' = \sqrt{N}\tau$ is the new threshold.

The probability of false alarm of the test in (3.84) cannot be evaluated in closed form for $N' > N$. This is because when $N' > N$, the samples of the DFT vector become correlated. A rough approximation however is the false alarm value when $N' = N$. Let $\hat{y}_k = \boldsymbol{\xi}^*(\frac{2\pi k}{N})\mathbf{y}$ be the value of k-th bin of the N-point DFT of $\mathbf{y}$. The approximation to probability of false alarm can be calculated as

$$\begin{aligned}
P_{\text{FA}} &= \Pr\left\{ \max_{k \in \mathcal{K}_{N'}} \left| \boldsymbol{\xi}^*\left(\frac{2\pi k}{N'}\right) \mathbf{y} \right| > \tau' \mid H_0 \right\} \\
&= 1 - \Pr\left\{ \max_{k \in \mathcal{K}_{N'}} \left| \boldsymbol{\xi}^*\left(\frac{2\pi k}{N'}\right) \mathbf{y} \right| \leq \tau' \mid H_0 \right\} \\
&\approx 1 - \Pr\left\{ |\hat{y}_k| \leq \tau' \text{ for } k \in \mathcal{K}_N \mid H_0 \right\} \\
&= 1 - \prod_{k \in \mathcal{K}_N} \Pr\left\{ |\hat{y}_k| \leq \tau' \mid H_0 \right\}
\end{aligned} \tag{3.85}$$

The last line in (3.85) is true because elements of $\hat{y}$ are independent random variables for H_0.

$\Pr\{|\hat{y}_k| \leq \tau' \mid H_0\}$ is known from the previous section. Therefore

$$P_{\text{FA}} \approx 1 - \prod_{k \in \mathcal{K}_N} \left\{ 1 - \exp\left(\frac{-\tau^2}{\sigma^2} \right) \right\}$$
$$= 1 - \left\{ 1 - \exp\left(\frac{-\tau^2}{\sigma^2} \right) \right\}^{|\mathcal{K}_N|} \tag{3.86}$$

where $|\mathcal{K}_N|$ is the number of elements of the set $\mathcal{K}_N$, or in other words the number of DFT frequency bins that are inside the expected frequency range of the signal. This approximation is equal to the exact value when $N' = N$.

Figure 3.4 shows the difference between the rough approximation and simulation results for $N' = 4N$.

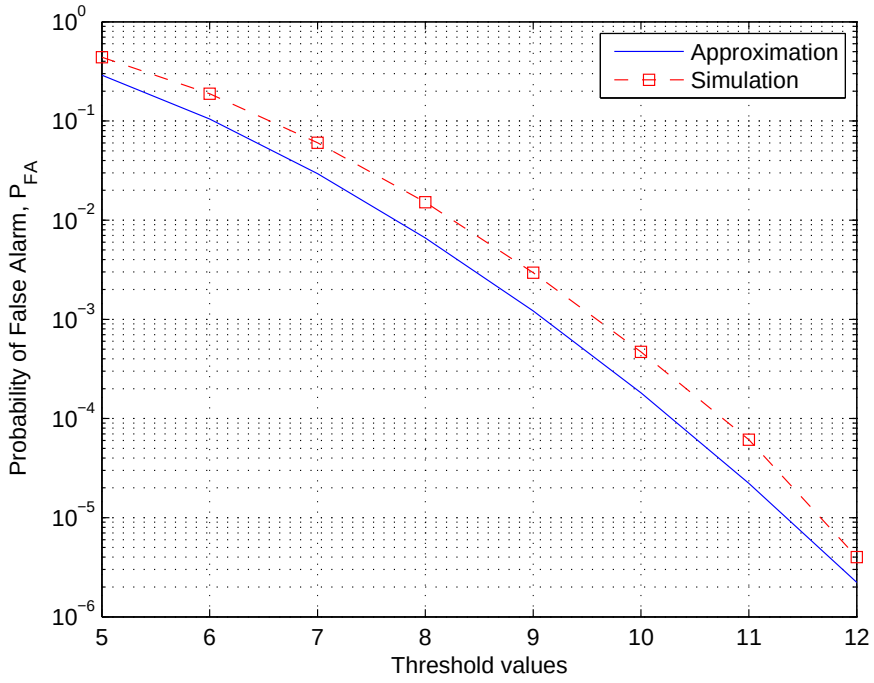

Figure 3.4: Approximation for probability of false alarm when $N' = 4N$

3.7 Detection of a Signal with Random Phase, Frequency and Length

Let the signal length $\underset{\sim}{N}$ be a random variable taking values from the set $\{1, 2, \ldots, M\}$ for a positive integer M. According to this length, the envelope $\mathbf{a}(\underset{\sim}{N}) \in \mathbb{C}^M$ of the signal is a

column vector with first $\underset{\sim}{N}$ elements nonzero. The other elements are bound to be zero. Also, in order to keep it independent of the total signal energy, it is normalized, that is

$$\|\mathbf{a}(\underset{\sim}{N})\|^2 = 1 \tag{3.87}$$

Now, the n-th element of the signal $\underset{\sim}{\mathbf{s}} \in \mathbb{C}^M$ can be defined as

$$\underset{\sim}{s}_n = \sqrt{E}\, a_n(\underset{\sim}{N})\, e^{j(\underset{\sim}{\omega} n + \underset{\sim}{\theta})} \quad \text{for } n = 0, 1, \ldots, M-1 \tag{3.88}$$

where

- $E \geq 0$ is the energy of the signal.
- $a_n(\underset{\sim}{N})$ is the n-th element of $\mathbf{a}(\underset{\sim}{N})$.
- $\underset{\sim}{\omega}$ defined in the interval $[0, 2\pi)$ with probability density function $p_{\underset{\sim}{\omega}}(.)$ is the radial frequency of the signal.
- $\underset{\sim}{\theta}$ which is uniformly distributed in the interval $[0, 2\pi)$ is the phase of the signal.

The frequency, phase and length are all independent of each other.

In vector notation, the signal can be represented as

$$\underset{\sim}{\mathbf{s}} = \sqrt{E}\, \mathbf{A}(\underset{\sim}{N})\, \boldsymbol{\xi}(\underset{\sim}{\omega})\, e^{j\underset{\sim}{\theta}} \tag{3.89}$$

where

- $\mathbf{A}(\underset{\sim}{N})$ is an M-by-M diagonal matrix with n-th diagonal element being equal to $a_n(\underset{\sim}{N})$.
- $\boldsymbol{\xi}(\underset{\sim}{\omega})$ is a column vector. Its n-th element is defined as

$$\xi_n(\underset{\sim}{\omega}) = e^{j\underset{\sim}{\omega} n} \quad \text{for } n = 0, 1, \ldots, M-1 \tag{3.90}$$

Note that calling E as the energy of the signal is valid since

$$\begin{aligned} \|\underset{\sim}{\mathbf{s}}\|^2 &= e^{-j\underset{\sim}{\theta}} \boldsymbol{\xi}^*(\underset{\sim}{\omega}) \mathbf{A}^*(\underset{\sim}{N})\, \sqrt{E}\, \sqrt{E} \mathbf{A}(\underset{\sim}{N}) \boldsymbol{\xi}(\underset{\sim}{\omega}) e^{j\underset{\sim}{\theta}} \\ &= E \|\mathbf{a}(\underset{\sim}{N})\|^2 \\ &= E \end{aligned} \tag{3.91}$$

Let the noise vector $\underset{\sim}{\mathbf{w}}$ be an M-dimensional circularly symmetric complex Gaussian vector with distribution $\mathcal{CN}(\mathbf{0}, \sigma^2\mathbf{I}_M)$.

By adapting equation (3.53) to the definition of the signal in this section

$$p_{\underset{\sim}{\mathbf{y}}}(\mathbf{y} \mid \underset{\sim}{\omega} = \omega, \underset{\sim}{N} = N, H_1) = \frac{1}{\pi^M \sigma^{2M}} \exp\left(-\frac{(\mathbf{y}^*\mathbf{y} + E)}{\sigma^2}\right) \mathcal{I}_0\left(\frac{2\sqrt{E}|\boldsymbol{\xi}^*(\omega)\mathbf{A}^*(N)\mathbf{y}|}{\sigma^2}\right) \tag{3.92}$$

Let $\mathcal{W}$ be a subset of $[0, 2\pi)$ and $\mathfrak{N}$ be a subset of $\mathbb{Z}^+$. If the probability densities of $\underset{\sim}{\omega}$ and $\underset{\sim}{N}$ are uniform in $\mathcal{W}$ and $\mathfrak{N}$ respectively and zero otherwise, then, using a similiar procedure in obtaining (3.80)

$$(\hat{\omega}, \hat{N}) = \arg \max_{\substack{\omega \in \mathcal{W} \\ N \in \mathfrak{N}}} \{|\boldsymbol{\xi}^*(\omega)\mathbf{A}^*(N)\mathbf{y}|\} \tag{3.93}$$

The test derived from the generalized likelihood ratio is similiar to (3.81):

$$\max_{\substack{\omega \in \mathcal{W} \\ N \in \mathfrak{N}}} \{|\boldsymbol{\xi}^*(\omega)\mathbf{A}^*(N)\mathbf{y}|\} > \tau \tag{3.94}$$

where τ is a threshold to be found from false alarm constraint.

3.8 Detection of a Signal with Random Phase, Frequency, Length and Delay

Let the delay time of the signal $\underset{\sim}{d}$ be a random variable taking values from the set $\{0, 1, \ldots, d_{\max}\}$ for a positive integer $d_{\max}$. Let the signal length $\underset{\sim}{N}$ be a random variable taking values from the set $\{1, 2, \ldots, N_{\max}\}$ for a positive integer $N_{\max}$. Let the length of the observation vector be M. Let $M \geq d_{\max} + N_{\max}$. According to delay and length, the envelope $\mathbf{a}(\underset{\sim}{d}, \underset{\sim}{N}) \in \mathbb{C}^M$ of the signal is a column vector with $\underset{\sim}{N}$ elements starting from the $\underset{\sim}{d}$-th element being nonzero. The other elements are bound to be zero. Also, in order to keep it independent of the total signal energy, it is normalized, that is

$$\|\mathbf{a}(\underset{\sim}{d}, \underset{\sim}{N})\|^2 = 1 \tag{3.95}$$

Now, the n-th element of the signal $\underset{\sim}{\mathbf{s}} \in \mathbb{C}^M$ can be defined as

$$\underset{\sim}{s}_n = \sqrt{E}\, a_n(\underset{\sim}{d}, \underset{\sim}{N})\, e^{j(\underset{\sim}{\omega} n + \underset{\sim}{\theta})} \quad \text{for } n = 0, 1, \ldots, M-1 \tag{3.96}$$

and in vector notation where

- $E \geq 0$ is the energy of the signal.

- $a_n(\underset{\sim}{d}, \underset{\sim}{N})$ is the n-th element of $\mathbf{a}(\underset{\sim}{d}, \underset{\sim}{N})$.
- $\underset{\sim}{\omega}$ defined in the interval $[0, 2\pi)$ with probability density function $p_{\underset{\sim}{\omega}}(.)$ is the radial frequency of the signal.
- $\underset{\sim}{\theta}$ which is uniformly distributed in the interval $[0, 2\pi)$ is the phase of the signal.

The frequency, phase, length and delay are all independent of each other.

In vector notation, the signal can be represented as

$$\underset{\sim}{\mathbf{s}} = \sqrt{E}\ \mathbf{A}(\underset{\sim}{d}, \underset{\sim}{N})\ \boldsymbol{\xi}(\underset{\sim}{\omega})\ e^{j\underset{\sim}{\theta}} \tag{3.97}$$

where

- $\mathbf{A}(\underset{\sim}{d}, \underset{\sim}{N})$ is an M-by-M diagonal matrix with n-th diagonal element being equal to $a_n(\underset{\sim}{N})$.
- $\boldsymbol{\xi}(\underset{\sim}{\omega})$ is a column vector. Its n-th element is defined as

$$\xi_n(\underset{\sim}{\omega}) = e^{j\underset{\sim}{\omega} n} \quad \text{for } n = 0, 1, \ldots, M-1 \tag{3.98}$$

Let the noise vector $\underset{\sim}{\mathbf{w}}$ be an M-dimensional circularly symmetric complex Gaussian vector with distribution $\mathcal{CN}(\mathbf{0}, \sigma^2\mathbf{I}_M)$.

Let $\mathcal{W}$, $\mathfrak{D}$ and $\mathfrak{N}$ be subsets of $[0, 2\pi)$, $\mathbb{Z}^+ \cup \{0\}$ and $\mathbb{Z}^+$ respectively. If the probability densities of $\underset{\sim}{\omega}$, $\underset{\sim}{d}$ and $\underset{\sim}{N}$ are uniform in $\mathcal{W}$, $\mathfrak{D}$ and $\mathfrak{N}$ respectively and zero otherwise, then, using a similiar procedure in (3.80)

$$(\hat{\omega}, \hat{N}, \hat{d}) = \arg \max_{\substack{\omega \in \mathcal{W} \\ d \in \mathfrak{D} \\ N \in \mathfrak{N}}} \{|\boldsymbol{\xi}^*(\omega)\mathbf{A}^*(d, N)\mathbf{y}|\} \tag{3.99}$$

The test derived from the generalized likelihood ratio is similiar to (3.81):

$$\max_{\substack{\omega \in \mathcal{W} \\ d \in \mathfrak{D} \\ N \in \mathfrak{N}}} \{|\boldsymbol{\xi}^*(\omega)\mathbf{A}^*(d, N)\mathbf{y}|\} > \tau \tag{3.100}$$

where τ is a threshold to be found from false alarm constraint.

CHAPTER 4

FURTHER ANALYSIS ON ROC CURVES

4.1 Introduction

The previous chapter suggested the detector to be used with random phase and frequency as the DFT detector. In the first of the following sections, an approximation is done for the probability of detection for the DFT detector. Noise is assumed to be white circularly symmetric complex Gaussian. Simulations show that when signal SNR increases, probability of detection approximation approach to its exact value.

In the other section, signal lenght is defined as random. The multiple window detector is used in this case. The exact values for the probability of false alarms are derived and an approximation for the probability of detection is compared with the simulation results.

4.2 Detector for a Signal with Random Phase and Frequency

Probability of detection can be approximated as if the estimated value of the frequency comes from the closest DFT bin. One may expect this approximation will approach to the true value when SNR is high.

In this section, an approximation is derived for the probability of detection and a summary is given. The signal model and the detection problem used in this section is defined in section 3.5.

In section 3.5, the relation between the probability of detection and the threshold depends on the expected value and the variance of $\mathbf{a}^*\mathbf{y}$ under H_1. With the signal frequency being random,

we can make use of the same relation by observing the expected value and the variance of $\underset{\sim}{z} = \frac{1}{\sqrt{N}}\boldsymbol{\xi}^*\left(\frac{2\pi k}{N'}\right)\mathbf{y}$. $\underset{\sim}{z}$ is the value of the k'th DFT bin scaled by $1/\sqrt{N}$. If we replace $\underset{\sim}{\mathbf{y}}$ by its definition,

$$\underset{\sim}{z} = \boldsymbol{\xi}^*\left(\frac{2\pi k}{N'}\right)\left(\frac{\sqrt{E}}{N}\boldsymbol{\xi}(\omega)e^{j\theta} + \frac{1}{\sqrt{N}}\underset{\sim}{\mathbf{w}}\right) \tag{4.1}$$

The expected value of $\underset{\sim}{z}$ is

$$\begin{aligned}\mathrm{E}\left\{\underset{\sim}{z}\right\} &= \boldsymbol{\xi}^*\left(\frac{2\pi k}{N'}\right)\frac{\sqrt{E}}{N}\boldsymbol{\xi}(\omega)e^{j\theta} \\ &= \frac{\sqrt{E}e^{j\theta}}{N}\sum_{n=0}^{N-1} e^{j\left(\omega-\frac{2\pi k}{N'}\right)n}\end{aligned} \tag{4.2}$$

By [38] and with few adjustments

$$\mathrm{E}\left\{\underset{\sim}{z}\right\} = \begin{cases}\sqrt{E}e^{j\theta} & \text{if } \omega = \dfrac{2\pi k}{N'} \\ \dfrac{\sqrt{E}e^{j\theta}}{N}e^{j\frac{N-1}{2}\left(\omega-\frac{2\pi k}{N'}\right)}\dfrac{\sin\left(\frac{N}{2}\left(\omega-\frac{2\pi k}{N'}\right)\right)}{\sin\left(\frac{1}{2}\left(\omega-\frac{2\pi k}{N'}\right)\right)} & \text{otherwise}\end{cases} \tag{4.3}$$

The variance of $\underset{\sim}{z}$ is equal to σ^2.

Using the result of the previous section, when radial frequency of the signal is ω and the detector structure is DFT,

$$P_{\mathrm{D}}(\tau) = \begin{cases}\mathrm{Q}_1\left(\dfrac{\sqrt{2E}}{\sigma}, \dfrac{\sqrt{2\tau^2}}{\sigma}\right) & \text{if } \omega = \dfrac{2\pi k}{N'} \text{ for some } k \in \{k : \dfrac{2\pi k}{N'} \in \mathcal{W}\} \\ \mathrm{Q}_1\left(\dfrac{\sqrt{2E}}{\sigma}\dfrac{\sin\left(\frac{N}{2}\left(\omega-\frac{2\pi k}{N'}\right)\right)}{N\sin\left(\frac{1}{2}\left(\omega-\frac{2\pi k}{N'}\right)\right)}, \dfrac{\sqrt{2\tau^2}}{\sigma}\right) & \text{otherwise}\end{cases} \tag{4.4}$$

Therefore, performance decreases when frequency of the signal is far away from the closest DFT bin. However, when the distance between the frequency and a particular DFT bin is more than $\frac{\pi k}{N'}$, then the neighbour DFT bin becomes the closest bin. Therefore, whatever the value of the frequency is, there will always be a DFT bin that is closer than $\frac{\pi k}{N'}$. The worst case for the performance will occur when the signal frequency is at the middle of two bins, namely $\omega = \frac{2\pi k}{N'} \pm \frac{\pi}{N'}$. The performance will be best when frequency is at an exact DFT bin, namely, $\omega = \frac{2\pi k}{N'}$. For all possible frequencies, the detector performance will stay between these two values. Now, if we assume that the maximum value always comes from the bin that is closest

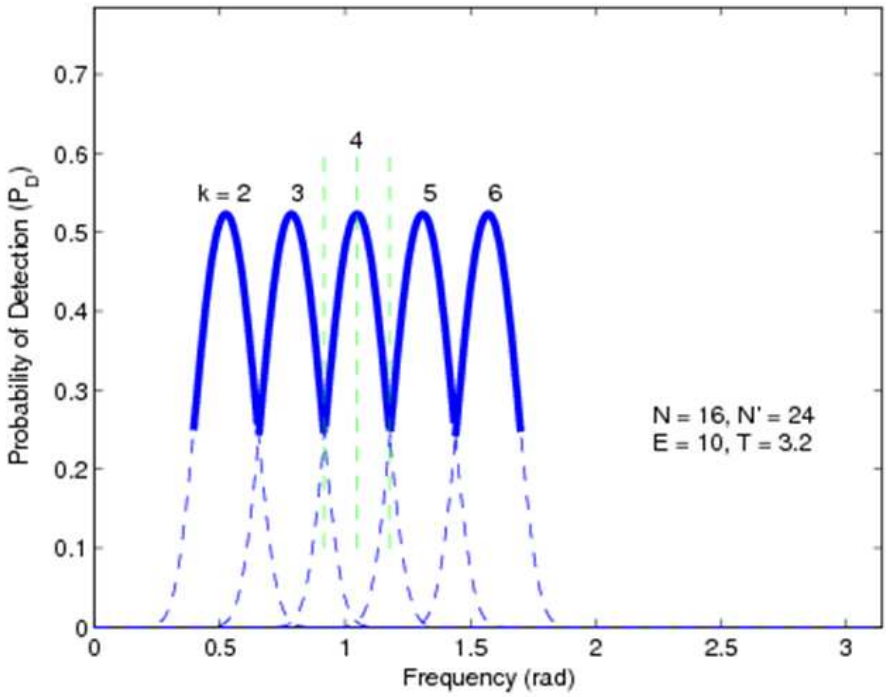

Figure 4.1: Probability of detection approximation vs. signal frequency for the DFT detector. Signal length is 16, DFT length is 24, energy of the signal is 10, detection threshold is 3.2.

to the actual frequency, the probability of detection can be approximated. This approximated probability of detection versus signal frequency can be observed in Figure 4.1.

With the above assumption, we can integrate the frequencies around the closest bin to find the probability of detection for random signal frequency. Mathematically,

$$P_{\mathrm{D}}(\tau) \approx \frac{N'}{2\pi} \int_{-\frac{\pi}{N'}}^{\frac{\pi}{N'}} \mathrm{Q}_1\left(\frac{\sqrt{2E}}{\sigma} \frac{\sin\left(\frac{N}{2}\left(\omega - \frac{2\pi k}{N'}\right)\right)}{N \sin\left(\frac{1}{2}\left(\omega - \frac{2\pi k}{N'}\right)\right)}, \frac{\sqrt{2\tau^2}}{\sigma} \right) \mathrm{d}\omega \tag{4.5}$$

Summary The detection problem in this section can be summarized as below.

$$\begin{aligned} H_0 &: \underset{\sim}{\mathbf{y}} \sim \mathcal{CN}\left(\mathbf{0}, \sigma^2 \mathbf{I}_N\right) \\ H_1 &: \underset{\sim}{\mathbf{y}} \sim \mathcal{CN}\left(\sqrt{E}\mathbf{A}\underset{\sim}{\boldsymbol{\xi}}(\omega)e^{j\theta}, \sigma^2 \mathbf{I}_N\right) \quad \text{given } \underset{\sim}{\theta} = \theta \text{ and } \underset{\sim}{\omega} = \omega \end{aligned} \tag{4.6}$$

The decision function based on GLRT:

$$\vartheta_{\mathrm{G}}(\mathbf{y}) = \begin{cases} 1 & \text{if } \max\limits_{k\in\mathcal{K}_{N'}} \left|\boldsymbol{\xi}^*\left(\frac{2\pi k}{N'}\right)\mathbf{A}^*\mathbf{y}\right| > \tau \\ 0 & \text{otherwise} \end{cases} \tag{4.7}$$

For the special case when $\mathbf{A}_{n,n} = \frac{1}{\sqrt{N}}$ for $n = 0, 1, \ldots, N-1$,

$$P_{\mathrm{FA}}(\tau) \approx 1 - \left\{1 - \exp\left(\frac{-\tau^2}{\sigma^2}\right)\right\}^{|\mathcal{K}_N|} \tag{4.8}$$

$$P_{\mathrm{D}}(\tau) \approx \frac{N'}{2\pi} \int_{-\frac{\pi}{N'}}^{\frac{\pi}{N'}} \mathrm{Q}_1\left(\sqrt{2\,\mathrm{SNR}}\frac{\sin\left(\frac{N}{2}\left(\omega - \frac{2\pi k}{N'}\right)\right)}{N\sin\left(\frac{1}{2}\left(\omega - \frac{2\pi k}{N'}\right)\right)}, \frac{\sqrt{2\tau^2}}{\sigma}\right) \mathrm{d}\omega \tag{4.9}$$

where

$$\mathrm{SNR} = \frac{E}{\sigma^2} \tag{4.10}$$

The simulated results together with the approximation is plotted in Figure 4.2. In the figure it can be seen that simulation results are always greater than the approximations, since some detections arise from DFT bins different from signal frequency. Another fact that approximations approach to the exact values for increasing SNR can also be seen in the figure.

4.3 Detector for a Signal with Random Phase and Length

Consider a case where only phase and length of the signal are random. Signal is defined as in (3.89) except the frequency is deterministic in this case. This case is analyzed further to find the probability of false alarm and approximate probability of detection. The reason to choose the frequency as nonrandom is to simplify the analysis. For the DFT detector detecting random frequency signals, previous results are used to extend the results for deterministic frequency.

The generalized likelihood ratio test for random phase and length is given as

$$\max_{N\in\mathfrak{N}} \{|\boldsymbol{\xi}^*(\omega)\mathbf{A}^*(N)\mathbf{y}|\} > \tau \tag{4.11}$$

That is calculate and threshold $|\boldsymbol{\xi}^*(\omega)\mathbf{A}^*(N)\mathbf{y}|$ for each possible N. If one of them exceeds the threshold, decide H_1, else decide H_0. The detector structure may be visualized as in Figure 4.3 where different length windows are working in parallel with the start time as 0.

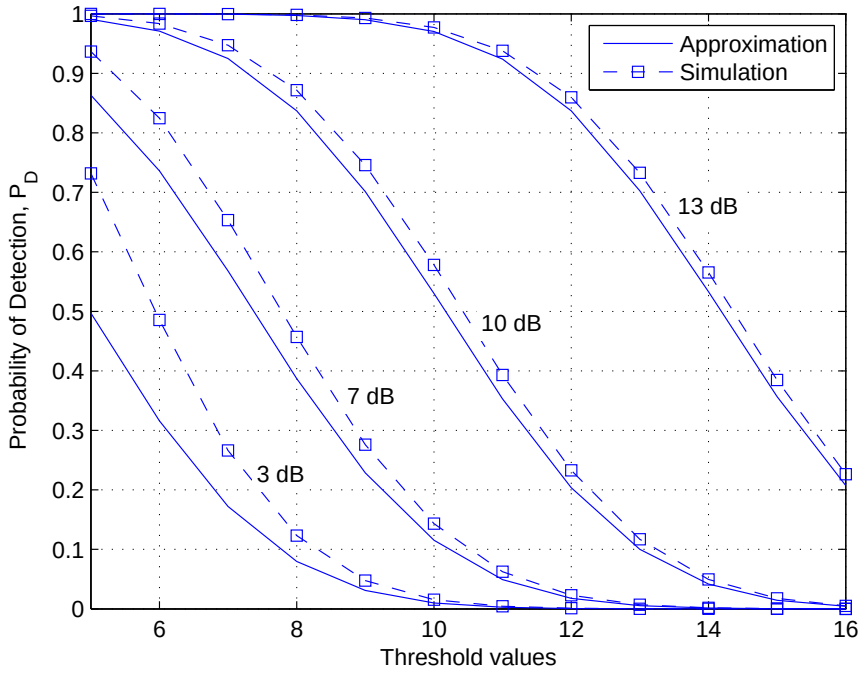

Figure 4.2: Probability of detection approximation for DFT detectors given in (4.9) together with simulation results.

For simplicity of calculations, choose the envelope of the signal to be rectangular. Namely,

$$\mathbf{A}_{n,n} = \frac{1}{\sqrt{N}} \quad \text{for } n = 0, 1, \ldots, N-1 \tag{4.12}$$

Now, the probability of false alarm will be analyzed. For this analysis, first it is required that the correlations between the different lengths be known. Let the variables $\underset{\sim}{z}_0, \underset{\sim}{z}_1, \ldots, \underset{\sim}{z}_{K-1}$ corresponding to different lengths $N_0 < N_1 < \ldots < N_{K-1}$ be defined as

$$\begin{aligned} \underset{\sim}{z}_0 &= \boldsymbol{\xi}^*(\omega)\mathbf{A}^*(N_0)\underset{\sim}{\mathbf{y}} \\ \underset{\sim}{z}_1 &= \boldsymbol{\xi}^*(\omega)\mathbf{A}^*(N_1)\underset{\sim}{\mathbf{y}} \\ &\vdots \\ \underset{\sim}{z}_{K-1} &= \boldsymbol{\xi}^*(\omega)\mathbf{A}^*(N_{K-1})\underset{\sim}{\mathbf{y}} \end{aligned} \tag{4.13}$$

where K is the number of different lengths to be evaluated. In matrix notation,

$$\underset{\sim}{\mathbf{z}} = \begin{bmatrix} \mathbf{A}(N_0)\boldsymbol{\xi}(\omega) & \mathbf{A}(N_1)\boldsymbol{\xi}(\omega) & \ldots & \mathbf{A}(N_{K-1})\boldsymbol{\xi}(\omega) \end{bmatrix}^* \underset{\sim}{\mathbf{y}} \tag{4.14}$$

where * corresponds to complex conjugate transpose of the matrix.

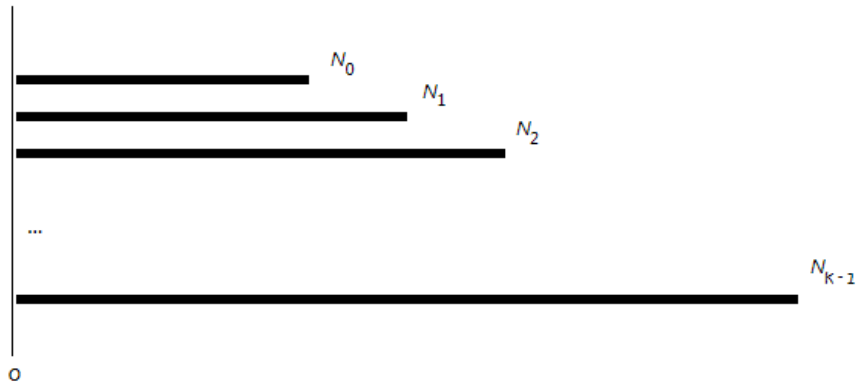

Figure 4.3: The detector multiple window structure.

If $\mathbf{W}_N(\omega)$ is an N-by-1 vector defined by its n-th element as

$$W_{N,n}(\omega) = e^{j\omega n} \text{ for } n = 0, 1, \ldots, N-1 \tag{4.15}$$

then,

$$\underset{\sim}{\mathbf{z}} = \begin{bmatrix} \frac{1}{\sqrt{N_0}}\mathbf{W}_{N_0}(\omega) & \frac{1}{\sqrt{N_1}}\mathbf{W}_{N_0}(\omega) & \cdots & \frac{1}{\sqrt{N_{K-1}}}\mathbf{W}_{N_0}(\omega) \\ 0 & \frac{1}{\sqrt{N_1}}\mathbf{W}_{(N_1-N_0)}(\omega)e^{jN_0\omega} & \cdots & \frac{1}{\sqrt{N_{K-1}}}\mathbf{W}_{(N_1-N_0)}(\omega)e^{jN_0\omega} \\ \vdots & \vdots & \vdots & \vdots \\ 0 & 0 & \cdots & \frac{1}{\sqrt{N_{K-1}}}\mathbf{W}_{(N_{K-1}-N_{K-2})}(\omega)e^{jN_{(K-2)}\omega} \end{bmatrix}^* \underset{\sim}{\mathbf{y}}' \tag{4.16}$$

where $\underset{\sim}{\mathbf{y}}'$ is an N_{K-1}-by-1 vector with elements equal to the first N_{K-1} elements of $\underset{\sim}{\mathbf{y}}$

For H_0, each $\underset{\sim}{z}_i$ is a zero mean complex Gaussian since it is a linear combination of $\mathbf{y}$. The

covariance matrix of $\underset{\sim}{\mathbf{z}}$ is then

$$
\begin{aligned}
\mathbf{\Gamma} = \mathrm{E}\left\{\underset{\sim}{\mathbf{z}}\underset{\sim}{\mathbf{z}}^*\right\} = \sigma^2 & \\
& \times \begin{bmatrix}
\frac{1}{\sqrt{N_0}}\mathbf{W}^*_{N_0}(\omega) & 0 & \dots & 0 \\
\frac{1}{\sqrt{N_1}}\mathbf{W}^*_{N_0}(\omega) & \frac{1}{\sqrt{N_1}}\mathbf{W}^*_{(N_1-N_0)}(\omega)e^{-jN_0\omega} & \dots & 0 \\
\vdots & \vdots & \vdots & \vdots \\
\frac{1}{\sqrt{N_{K-1}}}\mathbf{W}^*_{N_0}(\omega) & \frac{1}{\sqrt{N_{K-1}}}\mathbf{W}^*_{(N_1-N_0)}(\omega)e^{-jN_0\omega} & \dots & \frac{1}{\sqrt{N_{K-1}}}\mathbf{W}^*_{(N_{K-1}-N_{K-2})}(\omega)e^{-jN_{(K-2)}\omega}
\end{bmatrix} \\
& \times \begin{bmatrix}
\frac{1}{\sqrt{N_0}}\mathbf{W}_{N_0}(\omega) & \frac{1}{\sqrt{N_1}}\mathbf{W}_{N_0}(\omega) & \dots & \frac{1}{\sqrt{N_{K-1}}}\mathbf{W}_{N_0}(\omega) \\
0 & \frac{1}{\sqrt{N_1}}\mathbf{W}_{(N_1-N_0)}(\omega)e^{jN_0\omega} & \dots & \frac{1}{\sqrt{N_{K-1}}}\mathbf{W}_{(N_1-N_0)}(\omega)e^{jN_0\omega} \\
\vdots & \vdots & \vdots & \vdots \\
0 & 0 & \dots & \frac{1}{\sqrt{N_{K-1}}}\mathbf{W}_{(N_{K-1}-N_{K-2})}(\omega)e^{jN_{(K-2)}\omega}
\end{bmatrix} \\
& = \sigma^2 \\
& \times \begin{bmatrix}
\frac{1}{N_0}\mathbf{W}^*_{N_0}(\omega)\mathbf{W}_{N_0}(\omega) & \frac{1}{\sqrt{N_0N_1}}\mathbf{W}^*_{N_0}(\omega)\mathbf{W}_{N_0}(\omega) & \dots & \frac{1}{\sqrt{N_0N_{K-1}}}\mathbf{W}^*_{N_0}(\omega)\mathbf{W}_{N_0}(\omega) \\
\frac{1}{\sqrt{N_0N_1}}\mathbf{W}^*_{N_0}(\omega)\mathbf{W}_{N_0}(\omega) & \frac{1}{N_1}\mathbf{W}^*_{N_0}(\omega)\mathbf{W}_{N_0}(\omega) + \frac{1}{N_1}\mathbf{W}^*_{(N_1-N_0)}(\omega)\mathbf{W}_{(N_1-N_0)}(\omega) & \dots & \frac{1}{\sqrt{N_{K-1}}}\mathbf{W}^*_{N_0}(\omega)\mathbf{W}_{N_0}(\omega) \\
\vdots & \vdots & \dots & \frac{1}{\sqrt{N_{K-1}}}\mathbf{W}_{(N_1-N_0)}(\omega)e^{jN_0\omega} \\
0 & 0 & \vdots & \vdots \\
& & \dots & \frac{1}{\sqrt{N_{K-1}}}\mathbf{W}_{(N_{K-1}-N_{K-2})}(\omega)e^{jN_{(K-2)}\omega}
\end{bmatrix}
\end{aligned}
\tag{4.17}
$$

For another simplicity let ω satisfy

$$
\omega = \frac{2\pi k_0}{N_0} = \frac{2\pi k_1}{N_1} = \frac{2\pi k_2}{N_2} = \ldots = \frac{2\pi k_{(K-1)}}{N_{K-1}} \tag{4.18}
$$

for some integers $k_0, k_1, \ldots, k_{K-1}$. Note that this assumption also implies

$$
\omega = \frac{2\pi k'_1}{N_1 - N_0} = \frac{2\pi k'_2}{N_2 - N_1} = \ldots = \frac{2\pi k'_{K-1}}{N_{(K-1)} - N_{(K-2)}} \tag{4.19}
$$

for some integers $k'_0, k'_1, \ldots, k'_{K-1}$.

This choice of frequency allows the form of the covariance matrix to be simpler. Now,

$$\mathbf{\Gamma} = \sigma^2 \begin{bmatrix} 1 & \sqrt{\frac{N_0}{N_1}} & \sqrt{\frac{N_0}{N_2}} & \cdots & \sqrt{\frac{N_0}{N_{K-1}}} \\ \sqrt{\frac{N_0}{N_1}} & 1 & \sqrt{\frac{N_1}{N_2}} & \cdots & \sqrt{\frac{N_1}{N_{K-1}}} \\ \sqrt{\frac{N_0}{N_2}} & \sqrt{\frac{N_1}{N_2}} & 1 & \cdots & \sqrt{\frac{N_2}{N_{K-1}}} \\ \vdots & \vdots & \vdots & & \vdots \\ \sqrt{\frac{N_0}{N_{K-1}}} & \sqrt{\frac{N_1}{N_{K-1}}} & \sqrt{\frac{N_2}{N_{K-1}}} & \cdots & 1 \end{bmatrix} \tag{4.20}$$

The inverse of this matrix is interesting:

$$\begin{aligned} \mathbf{\Gamma}^{-1} &= \frac{1}{\sigma^2} \begin{bmatrix} \frac{N_1}{N_1-N_0} & -\frac{\sqrt{N_0N_1}}{N_1-N_0} & 0 & \cdots & 0 \\ -\frac{\sqrt{N_0N_1}}{N_1-N_0} & \frac{N_1}{N_1-N_0}+\frac{N_1}{N_2-N_1} & -\frac{\sqrt{N_1N_2}}{N_2-N_1} & \cdots & 0 \\ 0 & -\frac{\sqrt{N_1N_2}}{N_2-N_1} & \frac{N_2}{N_2-N_1}+\frac{N_2}{N_3-N_2} & \cdots & 0 \\ \vdots & \vdots & \vdots & & \vdots \\ 0 & 0 & 0 & \cdots & \frac{N_{K-1}}{N_{K-1}-N_{K-2}} \end{bmatrix} \\ &= \frac{1}{\sigma^2} \begin{bmatrix} \frac{N_1}{N_1-N_0} & -\frac{\sqrt{N_0N_1}}{N_1-N_0} & 0 & \cdots & 0 \\ -\frac{\sqrt{N_0N_1}}{N_1-N_0} & \frac{N_0}{N_1-N_0}+\frac{N_2}{N_2-N_1} & -\frac{\sqrt{N_1N_2}}{N_2-N_1} & \cdots & 0 \\ 0 & -\frac{\sqrt{N_1N_2}}{N_2-N_1} & \frac{N_1}{N_2-N_1}+\frac{N_3}{N_3-N_2} & \cdots & 0 \\ \vdots & \vdots & \vdots & & \vdots \\ 0 & 0 & 0 & \cdots & \frac{N_{K-1}}{N_{K-1}-N_{K-2}} \end{bmatrix} \end{aligned} \tag{4.21}$$

The inverse covariance matrix has nonzero elements only in the diagonal and lower and upper diagonals. With this result analytical forms for probability of false alarms can be derived easily.

The detector structure is composed of calculating and thresholding $|\boldsymbol{\xi}^*(\omega)\mathbf{A}^*(N)\mathbf{y}|$ for each possible N. However, for computational reasons, one may choose to evaluate that only at a few specific length values. In the following subsections, probability of false alarm is computed for a specific number of window lengths.

For H_0, $\underset{\sim}{\mathbf{z}}$ is a circularly symmetric complex Gaussian random vector since it is the result of a linear transformation of the circularly symmetric complex Gaussian random vector $\underset{\sim}{\mathbf{y}}$. Its covariance matrix and its inverse is given in (4.20) and (4.21) respectively.

The probability density function is

$$p_{\underset{\sim}{\mathbf{z}}}(\mathbf{z}) = \frac{1}{\pi^K \det(\mathbf{\Gamma})} \exp\left(\mathbf{z}^* \mathbf{\Gamma}^{-1} \mathbf{z}\right) \tag{4.22}$$

Let the elements of $\underset{\sim}{\mathbf{z}}$ be represented in polar coordinates such that

$$\underset{\sim}{z}_i = \underset{\sim}{r}_i e^{j\underset{\sim}{\phi}_i} \quad \text{for } i = 0, 1, \ldots, K-1. \tag{4.23}$$

Let $\underset{\sim}{\mathbf{r}}$ and $\underset{\sim}{\boldsymbol{\phi}}$ be K-dimensional vectors with i-th element equal to $\underset{\sim}{r}_i$ and $\underset{\sim}{\phi}_i$ respectively.

4.3.1 P_{FA} calculation using two windows

Here, an analytical form for the probability of false alarm is derived when the detector is composed of two windows with different lengths. We start with writing the joint probability density function for the magnitude and phase of the variable $|\boldsymbol{\xi}^*(\omega)\mathbf{A}^*(N)\mathbf{y}|$. Then by integrating out the phase components, we are left with the marginal probability density of the magnitudes. Then by finding the cumulative distribution evaluated at the desired threshold, we find a relationship between the threshold and the false alarm probability.

For $K = 2$, the covariance matrix and its inverse is

$$\boldsymbol{\Gamma} = \begin{bmatrix} \sigma^2 & \sigma^2\sqrt{\frac{N_0}{N_1}} \\ \sigma^2\sqrt{\frac{N_0}{N_1}} & \sigma^2 \end{bmatrix} \tag{4.24}$$

$$\boldsymbol{\Gamma}^{-1} = \begin{bmatrix} \frac{1}{\sigma^2}\frac{N_1}{N_1-N_0} & -\frac{1}{\sigma^2}\frac{\sqrt{N_0N_1}}{N_1-N_0} \\ -\frac{1}{\sigma^2}\frac{\sqrt{N_0N_1}}{N_1-N_0} & \frac{1}{\sigma^2}\frac{N_1}{N_1-N_0} \end{bmatrix} \tag{4.25}$$

Then, if we write the joint probability density function for the magnitudes and phases,

$$\begin{aligned} p_{\underset{\sim}{\mathbf{r}},\underset{\sim}{\boldsymbol{\phi}}}(\mathbf{r},\boldsymbol{\phi}) &= r_0 r_1 p_{\underset{\sim}{z}_0,\underset{\sim}{z}_1}\left(r_0 e^{j\phi_0}, r_1 e^{j\phi_1}\right) \\ &= \frac{1}{\sigma^4\pi^2}\frac{N_1}{N_1-N_0} r_0 r_1 \\ &\qquad \times \exp\left\{-\frac{N_1}{\sigma^2(N_1-N_0)}r_0^2 - \frac{N_1}{\sigma^2(N_1-N_0)}r_1^2 - \frac{2\sqrt{N_0N_1}}{\sigma^2(N_1-N_0)} r_0 r_1 \cos(\phi_0-\phi_1)\right\} \end{aligned} \tag{4.26}$$

The marginal probability density function of the magnitudes are

$$
\begin{aligned}
p_{\underline{r}_0,\underline{r}_1}(r_0,r_1) &= \int_0^{2\pi}\int_0^{2\pi} p_{\underline{\mathbf{r}},\underline{\boldsymbol{\phi}}}(\mathbf{r},\boldsymbol{\phi})\,\mathrm{d}\phi_0\mathrm{d}\phi_1 \\
&= \frac{1}{\sigma^4\pi^2}\frac{N_1}{N_1-N_0} r_0 r_1 \exp\left\{-\frac{N_1}{\sigma^2(N_1-N_0)}r_0^2 - \frac{N_1}{\sigma^2(N_1-N_0)}r_1^2\right\} \\
&\qquad\qquad \times \int_0^{2\pi}\int_0^{2\pi} \exp\left\{-\frac{2\sqrt{N_0N_1}}{\sigma^2(N_1-N_0)} r_0 r_1 \cos(\phi_0-\phi_1)\right\}\mathrm{d}\phi_0\mathrm{d}\phi_0 \\
&= \frac{4}{\sigma^4}\frac{N_1}{N_1-N_0} r_0 r_1 \exp\left\{-\frac{N_1}{\sigma^2(N_1-N_0)}r_0^2 - \frac{N_1}{\sigma^2(N_1-N_0)}r_1^2\right\} \mathcal{I}_0\left\{\frac{2\sqrt{N_0N_1}}{\sigma^2(N_1-N_0)} r_0 r_1\right\}
\end{aligned}
\tag{4.27}
$$

We can now proceed the calculation of P_{FA} as if $\sigma = 1$. The real value can be achieved by replacing τ with τ/σ. The probability of false alarm for a given threshold τ is

$$
\begin{aligned}
P_{\mathrm{FA}}(\tau) &= \Pr\{r_0 > \tau, r_1 > \tau \mid H_0\} \\
&= 1 - \Pr\{r_0 \le \tau, r_1 \le \tau \mid H_0\} \\
&= 1 - \frac{4N_1}{N_1-N_0}\int_0^{\tau}\int_0^{\tau} r_0 r_1 \exp\left\{-\frac{N_1}{N_1-N_0}r_0^2 - \frac{N_1}{N_1-N_0}r_1^2\right\}\mathcal{I}_0\left(\frac{2\sqrt{N_0N_1}}{N_1-N_0} r_0 r_1\right)\mathrm{d}r_0\mathrm{d}r_1 \\
&= 1 - \frac{4N_1}{N_1-N_0}\int_0^{\tau} r_1 e^{-r_1^2}\int_0^{\tau} r_0 \exp\left\{-\frac{N_1}{N_1-N_0}r_0^2 - \frac{N_0}{N_1-N_0}r_1^2\right\}\mathcal{I}_0\left(\frac{2\sqrt{N_0N_1}}{N_1-N_0} r_0 r_1\right)\mathrm{d}r_0\mathrm{d}r_1
\end{aligned}
\tag{4.28}
$$

We can solve this integral by defining a new dummy variable as

$$
u = \sqrt{\frac{2N_1}{N_1-N_0}}\, r_0 \tag{4.29}
$$

Then, integral inside becomes,

$$
\begin{aligned}
&\int_0^{\tau} r_0 \exp\left\{-\frac{N_1}{N_1-N_0}r_0^2 - \frac{N_0}{N_1-N_0}r_1^2\right\}\mathcal{I}_0\left(\frac{2\sqrt{N_0N_1}}{N_1-N_0} r_0 r_1\right)\mathrm{d}r_0 \\
&= \frac{N_1-N_0}{2N_1}\int_0^{\tau\sqrt{\frac{2N_1}{N_1-N_0}}} u \exp\left\{-\frac{1}{2}u^2 - \frac{N_0}{N_1-N_0}r_1^2\right\}\mathcal{I}_0\left(\sqrt{\frac{2N_0}{N_1-N_0}} r_1 u\right)\mathrm{d}u \\
&= \frac{N_1-N_0}{2N_1}\left[1 - \mathrm{Q}\left(\sqrt{\frac{2N_0}{N_1-N_0}} r_1, \tau\sqrt{\frac{2N_1}{N_1-N_0}}\right)\right]
\end{aligned}
\tag{4.30}
$$

Then, $P_{\mathrm{FA}}(\tau)$ is

$$P_{\mathrm{FA}}(\tau) = 1 - 2\int_0^{\tau} r_1 e^{-r_1^2}\left[1 - \mathrm{Q}\left(\sqrt{\frac{2N_0}{N_1-N_0}}r_1, \tau\sqrt{\frac{2N_1}{N_1-N_0}}\right)\right]\mathrm{d}r_1$$

$$= e^{-\tau^2} + \int_0^{\tau} 2r_1 e^{-r_1^2}\,\mathrm{Q}\left(\sqrt{\frac{2N_0}{N_1-N_0}}r_1, \tau\sqrt{\frac{2N_1}{N_1-N_0}}\right)\mathrm{d}r_1 \tag{4.31}$$

By [39],

$$\int_0^{\tau} 2r_1 e^{-r_1^2}\,\mathrm{Q}\left(\sqrt{\frac{2N_0}{N_1-N_0}}r_1, \tau\sqrt{\frac{2N_1}{N_1-N_0}}\right)\mathrm{d}r_1$$

$$= \int_0^{\infty} 2r_1 e^{-r_1^2}\,\mathrm{Q}\left(\sqrt{\frac{2N_0}{N_1-N_0}}r_1, \tau\sqrt{\frac{2N_1}{N_1-N_0}}\right)\mathrm{d}r_1$$

$$- \int_{\tau}^{\infty} 2r_1 e^{-r_1^2}\,\mathrm{Q}\left(\sqrt{\frac{2N_0}{N_1-N_0}}r_1, \tau\sqrt{\frac{2N_1}{N_1-N_0}}\right)\mathrm{d}r_1$$

$$= \mathrm{Q}\left(0, \tau\sqrt{\frac{2N_1}{N_1-N_0}}\right) + e^{-\tau^2} - e^{-\tau^2}\,\mathrm{Q}\left(0, \tau\sqrt{\frac{2N_0}{N_1-N_0}}\right)$$

$$- e^{-\tau^2}\,\mathrm{Q}\left(\tau\sqrt{\frac{2N_0}{N_1-N_0}}, \tau\sqrt{\frac{2N_1}{N_1-N_0}}\right) - e^{-\tau^2}$$

$$+ e^{-\tau^2}\,\mathrm{Q}\left(\tau\sqrt{\frac{2N_1}{N_1-N_0}}, \tau\sqrt{\frac{2N_0}{N_1-N_0}}\right)$$

$$= e^{-\tau^2}\left\{\mathrm{Q}\left(\tau\sqrt{\frac{2N_1}{N_1-N_0}}, \tau\sqrt{\frac{2N_0}{N_1-N_0}}\right) - \mathrm{Q}\left(\tau\sqrt{\frac{2N_0}{N_1-N_0}}, \tau\sqrt{\frac{2N_1}{N_1-N_0}}\right)\right\} \tag{4.32}$$

Finally,

$$P_{\mathrm{FA}}(\tau) = e^{-\tau^2} + e^{-\tau^2}\left\{\mathrm{Q}\left(\tau\sqrt{\frac{2N_1}{N_1-N_0}}, \tau\sqrt{\frac{2N_0}{N_1-N_0}}\right) - \mathrm{Q}\left(\tau\sqrt{\frac{2N_0}{N_1-N_0}}, \tau\sqrt{\frac{2N_1}{N_1-N_0}}\right)\right\} \tag{4.33}$$

Equation (4.33) gives the exact value for probability of false alarm for unity variance. For an arbitrary variance, replace τ by τ/σ

$$P_{\mathrm{FA}}(\tau) = e^{-\tau^2/\sigma^2}\left\{1 + \mathrm{Q}\left(\frac{\tau}{\sigma}\sqrt{\frac{2N_1}{N_1-N_0}}, \frac{\tau}{\sigma}\sqrt{\frac{2N_0}{N_1-N_0}}\right) - \mathrm{Q}\left(\frac{\tau}{\sigma}\sqrt{\frac{2N_0}{N_1-N_0}}, \frac{\tau}{\sigma}\sqrt{\frac{2N_1}{N_1-N_0}}\right)\right\} \tag{4.34}$$

This is the proability of false alarm for a two window detector structure with window lengths equal to N_0 and N_1 which satisfy $N_1 > N_0$. In figure 4.4, the theoretical result is compared with the simulation results.

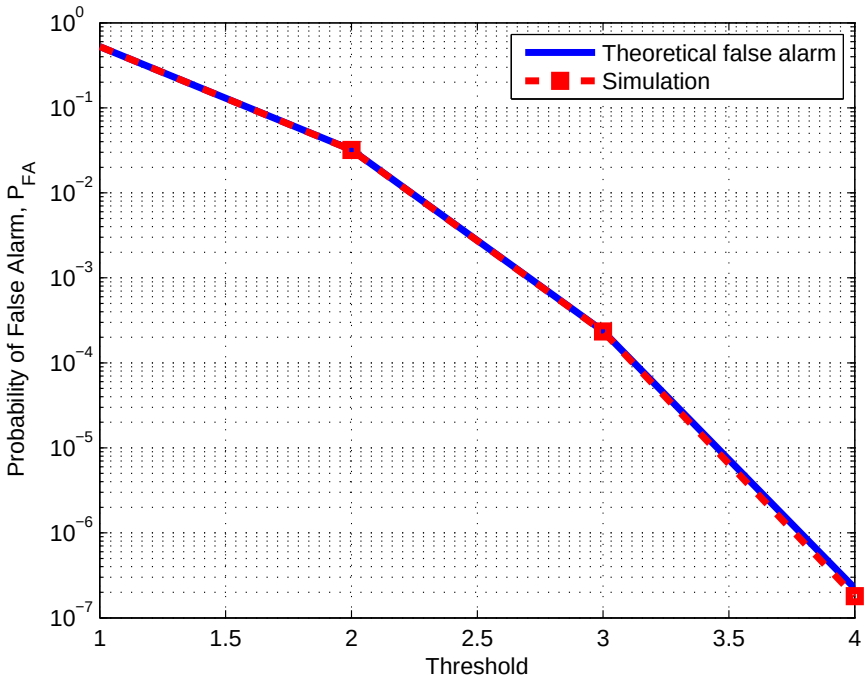

Figure 4.4: Comparison of the theoretical false alarm with results from simulation. Parameters are $\sigma = 1$, $N_0 = 16$ and $N_1 = 32$.

4.3.2 P_{FA} calculation using three windows

In the previous subsection, probability of false alarm for the two window detector was computed exactly. In this section, an exact form is calculated for 3 windows. The resultant P_{FA} form however contains a single integral to be evaluated numerically.

In order to derive P_{FA} for three windows, first a general form for the joint probability density function is written for 3 or more windows. Then the marginal probability density function is found for the magnitudes. A general form for the probability of false alarm is found for 3 or more windows. This general result is used for the specific $K = 3$ case.

The general joint probability density function for $K \geq 3$,

$$
\begin{aligned}
p_{\underset{\sim}{\mathbf{r}},\underset{\sim}{\boldsymbol{\phi}}}(\mathbf{r},\boldsymbol{\phi}) &= \left(\prod_{k=0}^{K-1} r_k\right) p_{\underset{\sim}{\mathbf{z}}}\left([r_0 e^{j\phi_0} r_1 e^{j\phi_1} \ldots r_{K-1} e^{j\phi_{K-1}}]^T\right) \\
&= \frac{1}{\pi^K}\left(\prod_{k=1}^{K-1}\frac{N_k}{N_k - N_{k-1}}\right)\left(\prod_{k=0}^{K-1} r_k\right)\exp\left\{-\frac{N_1}{N_1 - N_0}r_0^2 - \sum_{k=1}^{K-2}\left(\frac{N_{k-1}}{N_k - N_{k-1}} + \frac{N_{k+1}}{N_{k+1} - N_k}\right)r_k^2\right. \\
&\qquad \left. -\frac{N_{K-1}}{N_{K-1} - N_{K-2}}r_{K-1}^2 - 2\sum_{k=1}^{K-1}\frac{\sqrt{N_{k-1}N_k}}{N_k - N_{k-1}} r_k r_{k-1}\cos(\phi_k - \phi_{k-1})\right\} \qquad (4.35)
\end{aligned}
$$

The probability density function of the magnitudes are found by integrating out the phase components.

$$
\begin{aligned}
p_{\underset{\sim}{\mathbf{r}}}(\mathbf{r}) &= \int_0^{2\pi}\ldots\int_0^{2\pi} p_{\underset{\sim}{\mathbf{r}},\underset{\sim}{\boldsymbol{\phi}}}(\mathbf{r},\boldsymbol{\phi})\,\mathrm{d}\phi_0\mathrm{d}\phi_1\ldots\mathrm{d}\phi_{K-1} \\
&= \frac{1}{\pi^K}\left(\prod_{k=1}^{K-1}\frac{N_k}{N_k - N_{k-1}}\right)\left(\prod_{k=0}^{K-1} r_k\right)\exp\left\{-\frac{N_1}{N_1 - N_0}r_0^2 - \sum_{k=1}^{K-2}\left(\frac{N_{k-1}}{N_k - N_{k-1}} + \frac{N_{k+1}}{N_{k+1} - N_k}\right)r_k^2\right. \\
&\qquad \left. -\frac{N_{K-1}}{N_{K-1} - N_{K-2}}r_{K-1}^2\right\}\int_0^{2\pi}\ldots\int_0^{2\pi}\exp\left\{-2\sum_{k=1}^{K-1}\frac{\sqrt{N_{k-1}N_k}}{N_k - N_{k-1}} r_k r_{k-1}\cos(\phi_k - \phi_{k-1})\right\} \\
&\qquad\qquad \mathrm{d}\phi_0\mathrm{d}\phi_1\ldots\mathrm{d}\phi_{K-1} \\
&= 2^K\left(\prod_{k=1}^{K-1}\frac{N_k}{N_k - N_{k-1}}\right)\left(\prod_{k=0}^{K-1} r_k\right)\exp\left\{-\frac{N_1}{N_1 - N_0}r_0^2 - \sum_{k=1}^{K-2}\left(\frac{N_{k-1}}{N_k - N_{k-1}} + \frac{N_{k+1}}{N_{k+1} - N_k}\right)r_k^2\right. \\
&\qquad \left. -\frac{N_{K-1}}{N_{K-1} - N_{K-2}}r_{K-1}^2\right\}\prod_{k=1}^{K-1}\mathcal{I}_0\left(2\frac{\sqrt{N_{k-1}N_k}}{N_k - N_{k-1}} r_k r_{k-1}\right) \qquad (4.36)
\end{aligned}
$$

The probability of false alarm for a given threshold τ is

$$
\begin{aligned}
P_{\mathrm{FA}}(\tau) &= \Pr\{r_k > \tau \quad \text{for } k = 0, 1, \ldots, K-1 \mid H_0\} \\
&= 1 - \Pr\{r_k \leq \tau \quad \text{for } k = 0, 1, \ldots, K-1 \mid H_0\} \\
&= 1 - 2^K\left(\prod_{k=1}^{K-1}\frac{N_k}{N_k - N_{k-1}}\right)\int_0^{\tau}\ldots\int_0^{\tau}\left(\prod_{k=0}^{K-1} r_k\right) \\
&\times \exp\left\{-\frac{N_1}{N_1 - N_0}r_0^2 - \sum_{k=1}^{K-2}\left(\frac{N_{k-1}}{N_k - N_{k-1}} + \frac{N_{k+1}}{N_{k+1} - N_k}\right)r_k^2 - \frac{N_{K-1}}{N_{K-1} - N_{K-2}}r_{K-1}^2\right\} \\
&\times \prod_{k=1}^{K-1}\mathcal{I}_0\left(2\frac{\sqrt{N_{k-1}N_k}}{N_k - N_{k-1}} r_k r_{k-1}\right)\mathrm{d}r_0\mathrm{d}r_1\ldots\mathrm{d}r_{K-1} \qquad (4.37)
\end{aligned}
$$

The above is the general form for the probability of false alarm for detectors containing 3 or more windows. For the specific case when detector has 3 windows, a result containing a

single integral can be found. For $K = 3$,

$$
\begin{aligned}
P_{\mathrm{FA}}(\tau) &= 1 - 8\frac{N_1}{N_1 - N_0}\frac{N_2}{N_2 - N_1}\int_0^{\tau}\int_0^{\tau}\int_0^{\tau} r_0 r_1 r_2 \\
&\quad \times \exp\left\{-\frac{N_1}{N_1 - N_0}r_0^2 - \left(\frac{N_0}{N_1 - N_0} + \frac{N_2}{N_2 - N_1}\right)r_1^2 - \frac{N_2}{N_2 - N_1}r_2^2\right\} \\
&\quad \times \mathcal{I}_0\left(2\frac{\sqrt{N_0 N_1}}{N_1 - N_0}r_0 r_1\right)\mathcal{I}_0\left(2\frac{\sqrt{N_1 N_2}}{N_2 - N_1}r_1 r_2\right)\mathrm{d}r_0\mathrm{d}r_1\mathrm{d}r_2 \\
&= 1 - \frac{4N_2}{N_2 - N_1}\int_0^{\tau}\int_0^{\tau} r_1 r_2 \exp\left\{-\frac{N_2}{N_2 - N_1}r_1^2 - \frac{N_2}{N_2 - N_1}r_2^2\right\} \\
&\quad \times \mathcal{I}_0\left(2\frac{\sqrt{N_1 N_2}}{N_2 - N_1}r_1 r_2\right)\left[1 - \mathrm{Q}\left(\sqrt{\frac{2N_0}{N_1 - N_0}}r_1, \tau\sqrt{\frac{2N_1}{N_1 - N_0}}\right)\right]\mathrm{d}r_1\mathrm{d}r_2 \\
&= 1 - \frac{4N_2}{N_2 - N_1}\int_0^{\tau} r_1 e^{-r_1^2}\left[1 - \mathrm{Q}\left(\sqrt{\frac{2N_0}{N_1 - N_0}}r_1, \tau\sqrt{\frac{2N_1}{N_1 - N_0}}\right)\right] \\
&\quad \times \int_0^{\tau} r_2 \exp\left\{-\frac{N_1}{N_2 - N_1}r_1^2 - \frac{N_2}{N_2 - N_1}r_2^2\right\}\mathcal{I}_0\left(2\frac{\sqrt{N_1 N_2}}{N_2 - N_1}r_1 r_2\right)\mathrm{d}r_2\mathrm{d}r_1 \\
&= 1 - 2\int_0^{\tau} r_1 e^{-r_1^2}\left[1 - \mathrm{Q}\left(\sqrt{\frac{2N_0}{N_1 - N_0}}r_1, \tau\sqrt{\frac{2N_1}{N_1 - N_0}}\right)\right] \\
&\quad \times \left[1 - \mathrm{Q}\left(\sqrt{\frac{2N_1}{N_2 - N_1}}r_1, \tau\sqrt{\frac{2N_2}{N_2 - N_1}}\right)\right]\mathrm{d}r_1
\end{aligned}
\tag{4.38}
$$

The above relation is for unity variance. For an arbitrary variance,

$$
\begin{aligned}
P_{\mathrm{FA}}(\tau) &= 1 - 2\int_0^{\tau/\sigma} r_1 e^{-r_1^2}\left[1 - \mathrm{Q}\left(\sqrt{\frac{2N_0}{N_1 - N_0}}r_1, \frac{\tau}{\sigma}\sqrt{\frac{2N_1}{N_1 - N_0}}\right)\right] \\
&\quad \times \left[1 - \mathrm{Q}\left(\sqrt{\frac{2N_1}{N_2 - N_1}}r_1, \frac{\tau}{\sigma}\sqrt{\frac{2N_2}{N_2 - N_1}}\right)\right]\mathrm{d}r_1
\end{aligned}
\tag{4.39}
$$

This is the probability of false alarm for a detector containing 3 windows. In figure 4.5, the theoretical result is compared with the simulation results.

4.3.3 P_{FA} calculation using four windows

Here probability of false alarm is calculated for number of windows being equal to 4. The integrations first for r_0 and then for r_{K-1} are performed in the general form for $K \geq 3$. Then the specific case when $K = 4$ is written as a double integral form. This has to be numerically computed.

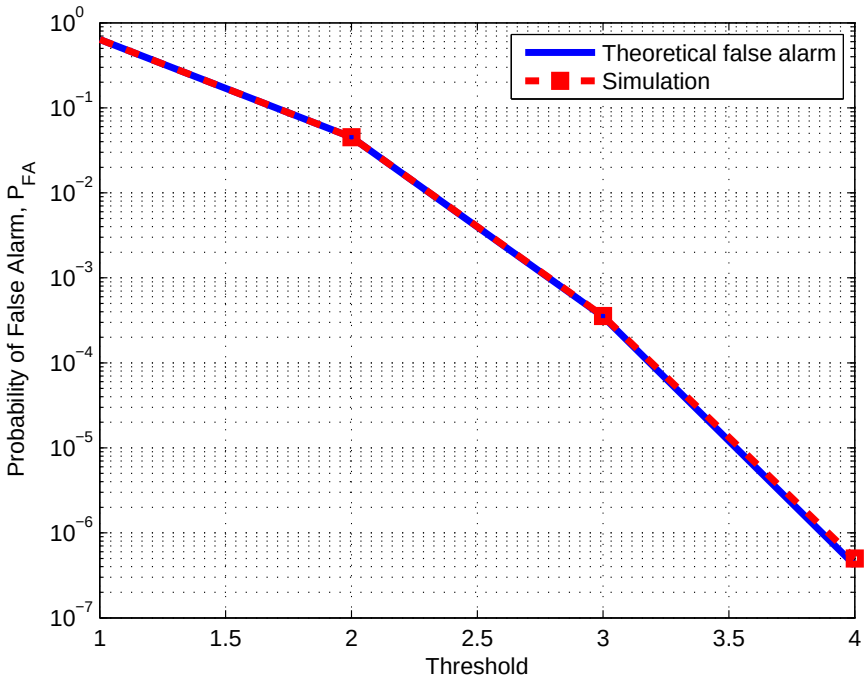

Figure 4.5: Comparison of the theoretical false alarm with results from simulation. Parameters are $\sigma = 1$, $N_0 = 16$, $N_1 = 32$ and $N_2 = 64$.

For $K \geq 4$

$$
\begin{aligned}
P_{\mathrm{FA}}(\tau) = 1 - 2^{K-1} & \left(\prod_{k=2}^{K-1} \frac{N_k}{N_k - N_{k-1}} \right) \int_0^{\tau} \cdots \int_0^{\tau} \left(\prod_{k=1}^{K-1} r_k \right) \\
& \times \exp\left\{ -\frac{N_2}{N_2 - N_1} r_1^2 - \sum_{k=2}^{K-2} \left(\frac{N_{k-1}}{N_k - N_{k-1}} + \frac{N_{k+1}}{N_{k+1} - N_k} \right) r_k^2 - \frac{N_{K-1}}{N_{K-1} - N_{K-2}} r_{K-1}^2 \right\} \\
& \times \left\{ \prod_{k=2}^{K-1} \mathcal{I}_0 \left(-2 \frac{\sqrt{N_{k-1} N_k}}{N_k - N_{k-1}} r_k r_{k-1} \right) \right\} \left[1 - \mathrm{Q}\left(\sqrt{\frac{2N_0}{N_1 - N_0}} r_1, \tau \sqrt{\frac{2N_1}{N_1 - N_0}} \right) \right] \\
& \times \mathrm{d}r_1 \ldots \mathrm{d}r_{K-1}
\end{aligned}
\tag{4.40}
$$

$$
\begin{aligned}
&= 1 - 2^{K-1}\left(\prod_{k=2}^{K-1}\frac{N_k}{N_k - N_{k-1}}\right)\int_0^{\tau}\cdots\int_0^{\tau}\left(\prod_{k=1}^{K-2} r_k\right)\\
&\quad\times\exp\left\{-\frac{N_2}{N_2-N_1}r_1^2 - \sum_{k=2}^{K-3}\left(\frac{N_{k-1}}{N_k - N_{k-1}} + \frac{N_{k+1}}{N_{k+1}-N_k}\right)r_k^2 - \frac{N_{K-3}}{N_{K-2}-N_{K-3}}r_{K-2}^2\right\}\\
&\quad\times\left\{\prod_{k=2}^{K-2}\mathcal{I}_0\left(2\frac{\sqrt{N_{k-1}N_k}}{N_k - N_{k-1}}r_k r_{k-1}\right)\right\}\left[1 - \mathrm{Q}\left(\sqrt{\frac{2N_0}{N_1-N_0}}r_1, \tau\sqrt{\frac{2N_1}{N_1-N_0}}\right)\right]\\
&\quad\times\int_0^{\tau} r_{K-1}\exp\left\{-\frac{N_{K-1}}{N_{K-1}-N_{K-2}}r_{K-2}^2 - \frac{N_{K-1}}{N_{K-1}-N_{K-2}}r_{K-1}^2\right\}\\
&\qquad\qquad\times\mathcal{I}_0\left(2\frac{\sqrt{N_{K-2}N_{K-1}}}{N_{K-1}-N_{K-2}}r_{K-1}r_{K-2}\right)\mathrm{d}r_{K-1}\\
&\qquad\qquad\times\mathrm{d}r_1\ldots\mathrm{d}r_{K-2}
\end{aligned}
\tag{4.41}
$$

$$
\begin{aligned}
&= 1 - 2^{K-2}\left(\prod_{k=2}^{K-2}\frac{N_k}{N_k - N_{k-1}}\right)\int_0^{\tau}\cdots\int_0^{\tau}\left(\prod_{k=1}^{K-2} r_k\right)\\
&\quad\times\exp\left\{-\frac{N_2}{N_2-N_1}r_1^2 - \sum_{k=2}^{K-3}\left(\frac{N_{k-1}}{N_k - N_{k-1}} + \frac{N_{k+1}}{N_{k+1}-N_k}\right)r_k^2 - \frac{N_{K-2}}{N_{K-2}-N_{K-3}}r_{K-2}^2\right\}\\
&\quad\times\prod_{k=2}^{K-2}\mathcal{I}_0\left(2\frac{\sqrt{N_{k-1}N_k}}{N_k - N_{k-1}}r_k r_{k-1}\right)\\
&\quad\times\left[1 - \mathrm{Q}\left(\sqrt{\frac{2N_0}{N_1-N_0}}r_1, \tau\sqrt{\frac{2N_1}{N_1-N_0}}\right)\right]\\
&\quad\times\left[1 - \mathrm{Q}\left(\sqrt{\frac{2N_{K-2}}{N_{K-1}-N_{K-2}}}r_{K-2}, \tau\sqrt{\frac{2N_{K-1}}{N_{K-1}-N_{K-2}}}\right)\right]\\
&\quad\times\mathrm{d}r_1\ldots\mathrm{d}r_{K-2}
\end{aligned}
\tag{4.42}
$$

For $K = 4$ and for an arbitrary variance,

$$
\begin{aligned}
P_{\mathrm{FA}}(\tau) &= 1 - 4\int_0^{\tau/\sigma}\int_0^{\tau/\sigma} r_1 r_2\exp\left\{-\frac{N_2}{N_2-N_1}r_1^2 - \frac{N_2}{N_2-N_1}r_2^2\right\}\mathcal{I}_0\left(2\frac{\sqrt{N_1N_2}}{N_2-N_1}r_1 r_2\right)\\
&\quad\times\left[1 - \mathrm{Q}\left(\sqrt{\frac{2N_0}{N_1-N_0}}r_1, \frac{\tau}{\sigma}\sqrt{\frac{2N_1}{N_1-N_0}}\right)\right]\left[1 - \mathrm{Q}\left(\sqrt{\frac{2N_2}{N_3-N_2}}r_2, \frac{\tau}{\sigma}\sqrt{\frac{2N_3}{N_3-N_2}}\right)\right]\mathrm{d}r_1\mathrm{d}r_2
\end{aligned}
\tag{4.43}
$$

In figure 4.6, the theoretical result is compared with the simulation results.

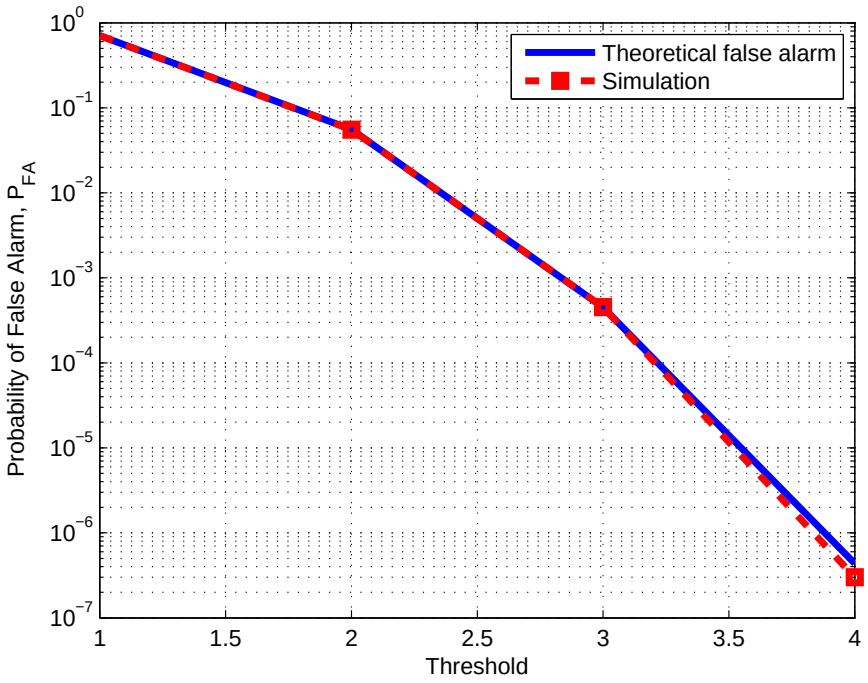

Figure 4.6: Comparison of the theoretical false alarm with results from simulation. Parameters are $\sigma = 1$, $N_0 = 16$, $N_1 = 32$, $N_2 = 64$ and $N_3 = 96$.

4.3.4 Approximation for probability of detection

An approximation can be made for probability of detection with the assumption that $\hat{N}$ is equal to the actual signal length.

The assumption here is that the observer system knows the possible values for the signal length. For example it knows that the signal length will be one of $N_0 = 16$, $N_1 = 32$, $N_2 = 64$ or $N_3 = 96$ with equal probability. The detector is also composed of 4 windows with the same lengths in this example. If it is assumed that when a detection occurs, this detection comes from the window with the length equal to the signal's length, calculation of the probability of detection is easy. One can expect that this assumption is true for most of the time when the signal power is much higher than the noise power.

Let

$$\underset{\sim}{z} = |\boldsymbol{\xi}^*(\omega)\mathbf{A}^*(\hat{N})\underset{\sim}{\mathbf{y}}| \tag{4.44}$$

For H_1, $2\tilde{z}^2/\sigma^2$ is noncentral chi-square distributed with 2 degrees of freedom and with non-centrality parameter $2E/\sigma^2$.

$$\begin{aligned} P_{\mathrm{D}}(\tau) &\approx \Pr\left\{\tilde{z} > \tau \mid H_1\right\} \\ &= 1 - \Pr\left\{\tilde{z} \le \tau \mid H_1\right\} \\ &= 1 - \Pr\left\{2\tilde{z}^2/\sigma^2 \le 2\tau^2/\sigma^2 \mid H_1\right\} \\ &= 1 - \mathrm{F}_{\chi^2}(2\tau^2/\sigma^2, 2\,\mathrm{SNR}) \end{aligned} \tag{4.45}$$

where $\mathrm{F}_{\chi^2}(.,\lambda)$ is the cumulative distribution function of a noncentral chi-square distribution of 2 degrees of freedom with non-centrality parameter of λ. The SNR definition is E/σ^2.

In Figure 4.7, the approximation is compared with the simulation results. As seen from the figure, for high SNR, the approximation is closer to the actual value since the estimation value of the length is more likely to be correct. The actual value of the probability of detection must be higher than the approximated value since there is always a possibility of detection from the other windows. The figure illustrates this idea.

When due to computational reasons, the window count in the detector is less than all the possible lengths of the signal, then probability of detection may be approximated again by assuming the length estimate (which equals to one of the windows in the detector) is the one that gives the highest detection result individually.

For H_1, and for signal length N_s,

$$\begin{aligned} \mathrm{E}\left\{\tilde{z}\right\} &= \boldsymbol{\xi}^*(\omega)\mathbf{A}^*(\hat{N})\sqrt{E}\mathbf{A}(N_s)\boldsymbol{\xi}(\omega)e^{j\theta} \\ &= \begin{cases} \sqrt{\dfrac{N_s E}{\hat{N}}}e^{j\theta} & \text{if } \hat{N} \ge N_s \\ \sqrt{\dfrac{\hat{N}E}{N_s}}e^{j\theta} & \text{otherwise} \end{cases} \end{aligned} \tag{4.46}$$

Using previous results,

$$P_{\mathrm{D}}(\tau) = \begin{cases} \mathrm{Q}_1\left(\sqrt{\dfrac{2N_sE}{\hat{N}\sigma^2}}, \dfrac{\sqrt{2\tau^2}}{\sigma}\right) & \text{if } \hat{N} \ge N_s \\ \mathrm{Q}_1\left(\sqrt{\dfrac{2\hat{N}E}{N_s\sigma^2}}, \dfrac{\sqrt{2\tau^2}}{\sigma}\right) & \text{otherwise} \end{cases} \tag{4.47}$$

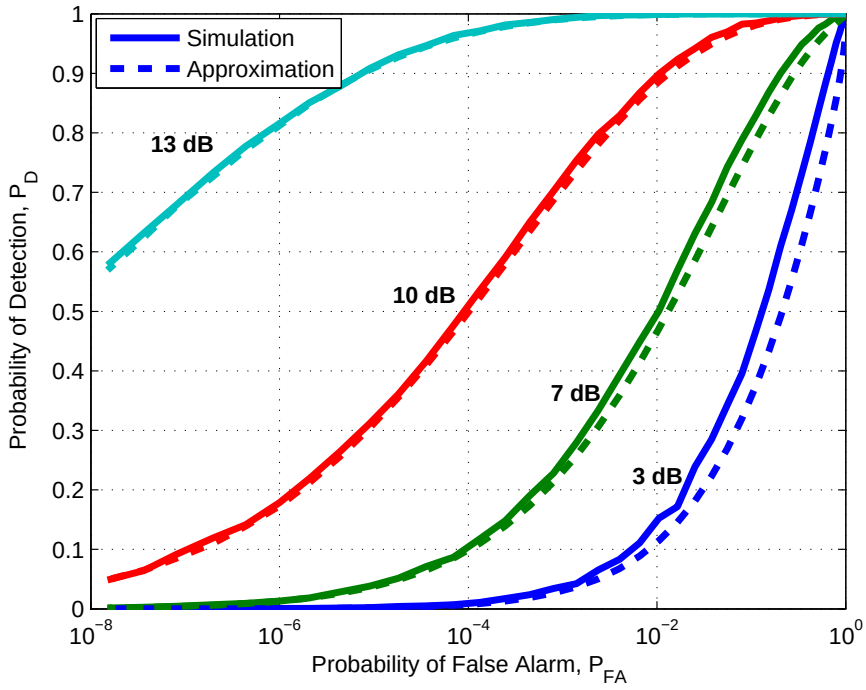

Figure 4.7: Comparison of the approximated probability of detection and simulation results. Parameters are $\sigma = 1$, $N_0 = 16$, $N_1 = 32$, $N_2 = 64$ and $N_3 = 96$.

Let $N_{\mathrm{l}}(N_s) = \max\{N : N \leq N_s\}$ and $N_{\mathrm{r}}(N_s) = \min\{N : N > N_s\}$. That is N_{l} is the window with length closest to N_s but less than N_s and N_{r} is the window with length closest to N_s but higher than N_s. Now, using the assumption that the length estimate is the window that gives the highest detection result individually,

$$P_{\mathrm{D}}(\tau) \approx \mathrm{Q}_1\left(\frac{\sqrt{2E}}{\sigma}\sqrt{\max\left(\frac{N_{\mathrm{l}}(N_s)}{N_s}, \frac{N_s}{N_{\mathrm{r}}(N_s)}\right)}, \frac{\sqrt{2\tau^2}}{\sigma}\right) \tag{4.48}$$

When signal length is uniformly distributed in a domain $\mathfrak{N}$,

$$P_{\mathrm{D}}(\tau) \approx \int_{\mathfrak{N}} \mathrm{Q}_1\left(\frac{\sqrt{2E}}{\sigma}\sqrt{\max\left(\frac{N_{\mathrm{l}}(N)}{N}, \frac{N}{N_{\mathrm{r}}(N)}\right)}, \frac{\sqrt{2\tau^2}}{\sigma}\right) p_{\tilde{N}}(N)\,\mathrm{d}N \tag{4.49}$$

Figure 4.8 shows the approximation given in (4.49) together with simulation result. Figure 4.9 shows the performance of some multiple window detectors together.

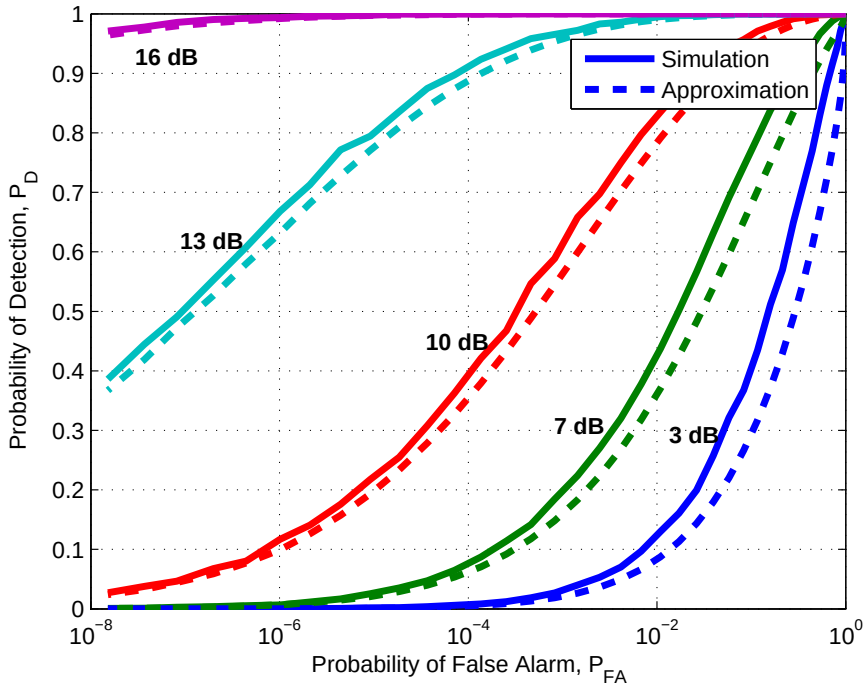

Figure 4.8: Comparison of simulation results with approximation for probability of detection

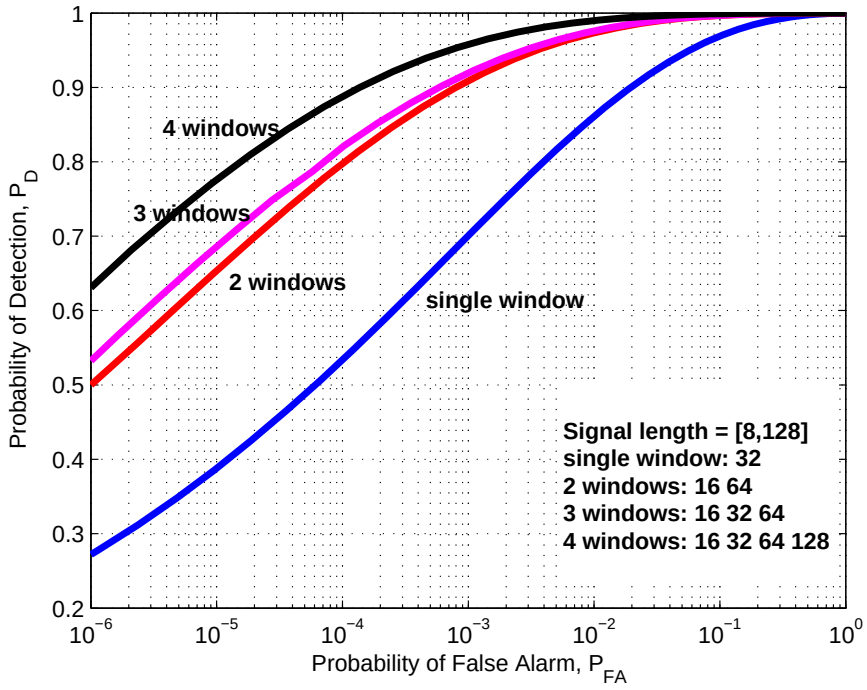

Figure 4.9: Comparison of multiple window detectors for SNR=13dB

Summary The detection problem in this section can be summarized as below.

$$\begin{aligned} H_0 &: \underset{\sim}{\mathbf{y}} \sim \mathcal{CN}\left(\mathbf{0}, \sigma^2 \mathbf{I}_M\right) \\ H_1 &: \underset{\sim}{\mathbf{y}} \sim \mathcal{CN}\left(\sqrt{E}\mathbf{A}(N)\boldsymbol{\xi}(\omega)e^{j\theta}, \sigma^2 \mathbf{I}_M\right) \quad \text{given } \underset{\sim}{\theta} = \theta \text{ and } \underset{\sim}{N} = N \end{aligned} \tag{4.50}$$

The decision function based on GLRT:

$$\mathfrak{d}_{\mathrm{G}}(\mathbf{y}) = \begin{cases} 1 & \text{if } \max\limits_{N \in \mathfrak{N}} \{|\boldsymbol{\xi}^*(\omega)\mathbf{A}^*(N)\mathbf{y}|\} > \tau \\ 0 & \text{otherwise} \end{cases} \tag{4.51}$$

The probability of false alarm for a given threshold is given in the previous subsections.

For the special case when $\mathbf{A}_{n,n} = \frac{1}{\sqrt{N}}$ for $n = 0, 1, \ldots, N-1$, the probability of detection for a given threshold is approximated as

$$P_{\mathrm{D}}(\tau) \approx \int_{\mathfrak{N}} \mathrm{Q}_1\left(\frac{\sqrt{2E}}{\sigma}\sqrt{\max\left(\frac{N_{\mathrm{l}}(N)}{N}, \frac{N}{N_{\mathrm{r}}(N)}\right)}, \frac{\sqrt{2\tau^2}}{\sigma}\right) p_{\underset{\sim}{N}}(N)\,\mathrm{d}N \tag{4.52}$$

where

$$\mathrm{SNR} = \frac{E}{\sigma^2} \tag{4.53}$$

CHAPTER 5

SIMULATIONS FOR MULTIPLE WINDOWS

5.1 Brute Force Method of Finding Best Window Length

In Section 3.7, the detector structure based on GLRT for signals with random phase, frequency and length is given. In Section 4.3, probability of false alarm and probability detection are analyzed. When using a detector composed of multiple windows, with window count less than the number of possible signal length values, the question of which lengths to optimally choose for the detector remains unknown. In this section, some simulations are performed to estimate the optimal window lengths for some different cases. This is performed for different number of windows and it is shown by simulation that for the given examples, when the lengths are chosen as optimal, as the number of windows increase the overall probability of detection increases.

In the following subsections, some examples are given and simulations are performed for detectors different number of windows. In the last subsection, result are compared.

5.1.1 Best window length (single window)

The example consists of detecting a signal of 13 dB SNR with random length taking integer values and uniformly distributed between 8 and 128. The detector structure is the one given in Section 4.3 and rewritten here for convenience.

$$\max_{N\in\mathfrak{N}} \{|\boldsymbol{\xi}^*(\omega)\mathbf{A}^*(N)\mathbf{y}|\} > \tau \tag{5.1}$$

Simulations are performed for a probability of false alarm range from 10^{-8} to 1. Using brute force, P_{D} vs. P_{FA} were plotted for all possible detector according to window length. The

results can be seen in Figure 5.1. The red line marks the best P_D-P_{FA} curve. The result of this simulation says that when the designer is constrained to use only a single window for the detector, he/she must choose a window with length 73. This number is somehow close to the midpoint of the interval of possible signal lengths, that is $\frac{128+8}{2} = 68$

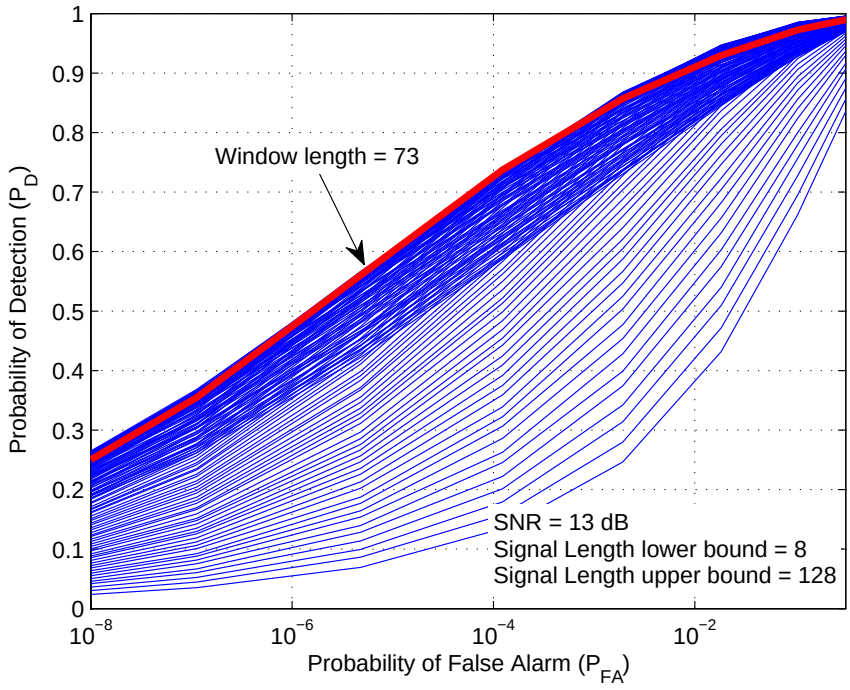

Figure 5.1: Best window length in terms of probability of detection. The detector is composed of a single window. Signal length is uniformly distributed between 8 and 128.

5.1.2 Best window lengths (two windows)

This subsection gives the results of the simulations similiar to the previous subsection with multiple window detector having two windows. Detection performances for some window combinations are simulated and the best pair is noted. Not all window combinations were simulated in order to keep simulation run time low. The simulated pairs are the ones that are not close to each other by some number. The results can be seen in Figure 5.2. The red line again marks the best P_D-P_{FA} curve. The result of this simulation says that when the designer is constrained to use only two windows for the detector, he/she must choose the lengths of the windows as 34 and 95. These numbers are somehow close to the numbers $8 + \frac{128-8}{4} = 38$ and

$8 + 3\frac{128-8}{4} = 98$. The numbers suggested are the one fourth and three fourth of the interval $[8, 128]$.

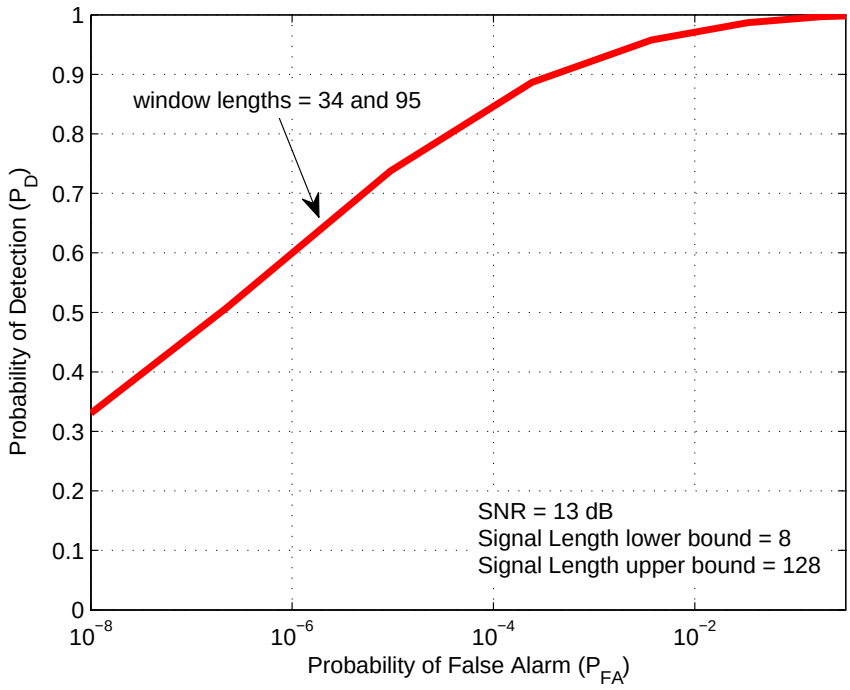

Figure 5.2: Best window lengths in terms of probability of detection. The detector is composed of two windows. Signal length is uniformly distributed between 8 and 128.

5.1.3 Best window lengths (three windows)

This subsection gives the results of the simulations similiar to the previous subsections with multiple window detector having three windows. The best P_{D}-P_{FA} curve is given in Figure 5.3. The result of this simulation says that when the designer is constrained to use only three windows for the detector, he/she must choose the lengths of the windows as 21, 58 and 104. These numbers are somehow close to the numbers $8 + \frac{128-8}{6} = 28$, $8 + 3\frac{128-8}{6} = 68$ and $8 + 5\frac{128-8}{6} = 108$. The numbers suggested are the one sixth, three sixth and five sixth of interval $[8, 128]$.

In the three subsections, some values are suggested which are in some sense close to optimal window lengths. The general formula for this suggestion is given below.

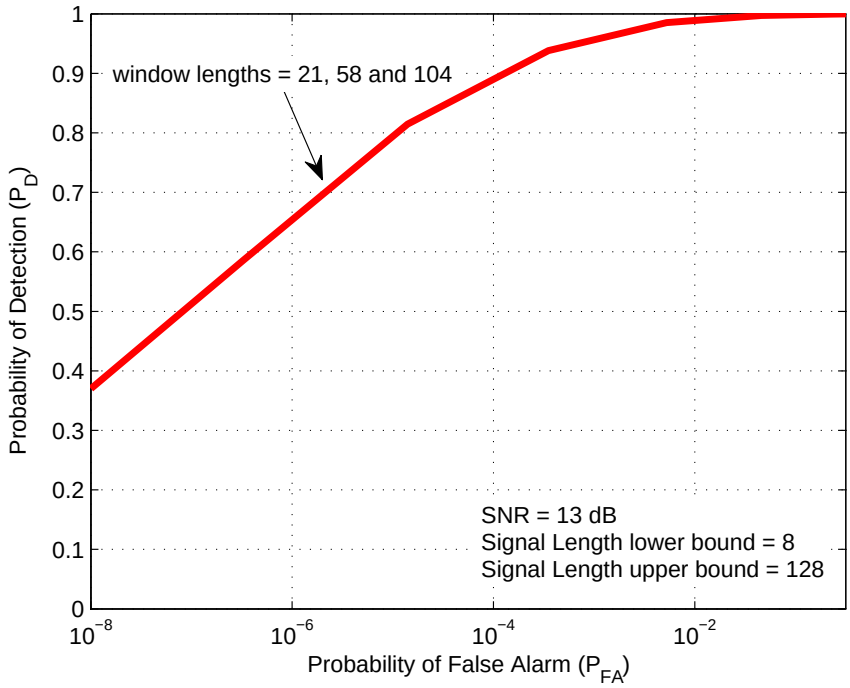

Figure 5.3: Best window lengths in terms of probability of detection. The detector is composed of three windows. Signal length is uniformly distributed between 8 and 128.

Let the signal length is a uniform random variable in the interval $[a, b]$. For a detector with K windows, the window lengths $N_0, N_1, \ldots, N_{K-1}$ can be chosen as

$$N_k = a + (2k+1)\frac{b-a}{2K} \qquad \text{for } k = 0, 1, \ldots, K-1 \tag{5.2}$$

that is divide the interval into $2K$ equal sections and set the window lengths to the end of 1st, 3rd, 5th, etc. sections.

This may be thought as a rule of thumb for the choice of window lengths and will give a performance that is somehow close to optimal.

5.1.4 Comparison of different length windows

In order to compare the best results for detectors having different number of windows, P_{D} vs. P_{FA} curves are plotted together as solid lines in Figure 5.4. The performance for the suggested values of the window lengths are given as dotted lines.

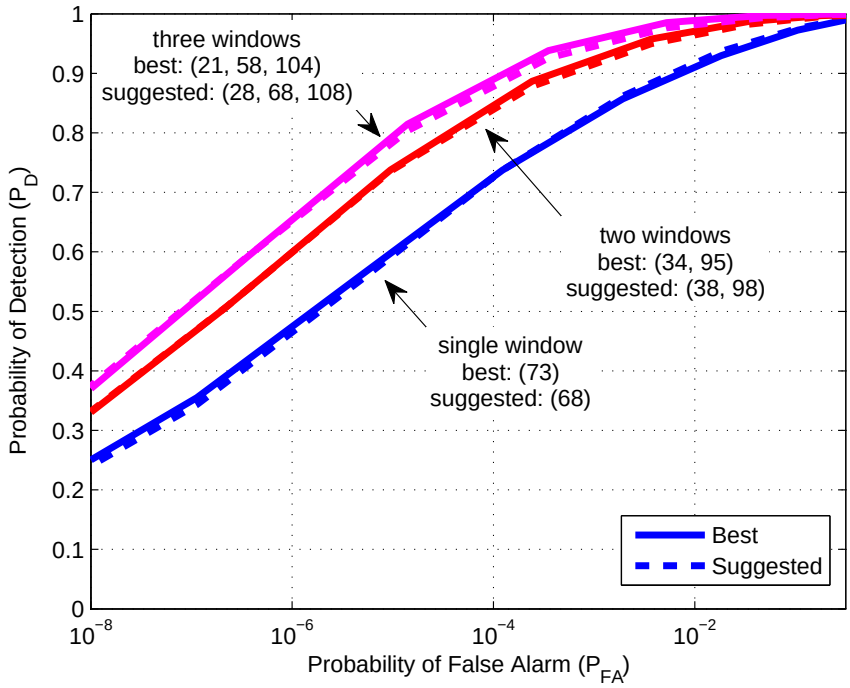

Figure 5.4: Comparison of performances of detectors with different number of windows.

As seen from the figure, as a simulation result, for this example, when the number of windows is increased the performance of the detector increases. Another result is the formula suggested in equation (5.2) gives close to optimal results.

5.2 Performance with Respect to Overlap Amount

When the signal length is a uniformly distributed random variable, the suitable detector is a multiple window detector. When the delay is also random, the GLRT detector is composed of overlapping windows in order to evaluate and threshold for each delay time. In this section, for a given example, it is shown that performance increases with increasing overlap.

The detectors give the best performance when the detector window length coincides with the signal. When the delay time of the signal is unknown, in order to guarantee that one window will match the signal, one must "slide" the windows one sample for each sample in the analysis interval. This way if window length and signal length are the same, one window will match the signal. In this case the overlap amount is one sample less than the whole

window length. With computational considerations one may decrease the overlap amount. In this case, according to signal delay there may be no windows matching the signal but one will cover most of it if the overlap is high enough. For instance when the overlap is 50 percent of the window, then for the worst case, a detection window will cover 75 percent of the signal.

Overlap of windows may be visualized as in Figure 5.5.

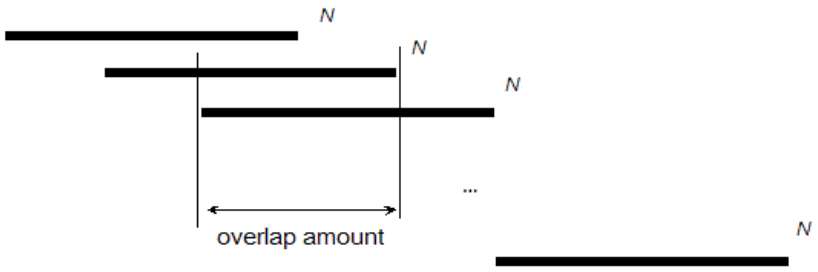

Figure 5.5: Structure of windows in overlapping window detector.

The simulation is performed for a 13 dB signal with length 16. Single window detectors with different overlaps are used. The plots for the P_D vs P_{FA} curves are given in Figure 5.6.

5.3 Simulations for a Nonconfined Analysis Interval

In a real life application, the receiver receives a sequence of signals in time and usually their initial time cannot be known exactly. The detector in this case consists of overlapping windows in a continuous basis. When the signal length is also random, then the detector must contain multiple windows. The detector will work continuously for each sample received. When enough samples come to fill a particular window of detector, the detection will be performed for that window. This process will go on for a nonconfined time interval.

When the detector is composed of overlapping multiple windows in a nonconfined interval, the traditional definition of probability of false alarm may not be suitable. Definition may be specific to an application. One definition can be as follows:

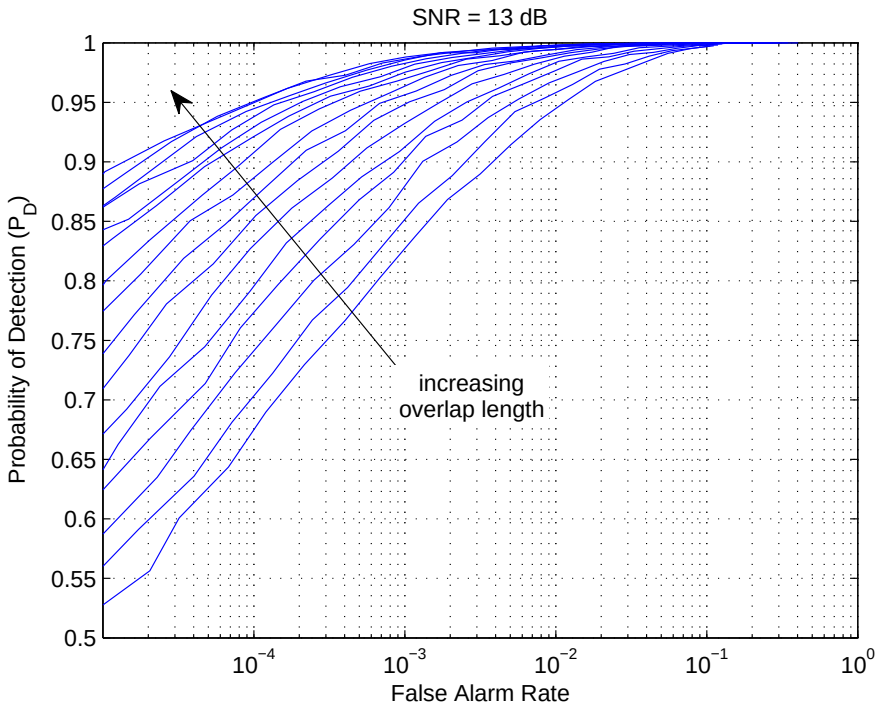

Figure 5.6: Relation between window overlaps and detection performance

Let there be no signal in the run time of the detector. Under this condition, let the false alarm interval be defined as the set of samples contained in all the windows in which a detection is made. Then the probability of false alarm may be defined as the ratio of the number of elements of false alarm interval to total run time when run time goes to infinity. The motivation behind this definition is to give more cost to the longer windows. In another application, for example, the costs for each window may be the same, and a different definition may be given.

In this framework, (where the signals are received as a sequence) if we say that a particular signal is detected, then this means that at least one of the windows intersecting that signal must give a detection.

With these definitions for signal detection and probability of false alarm, some simulations were performed for different detectors containing different overlaps and different number of windows. The results are given in Figures 5.7, 5.8 and 5.9.

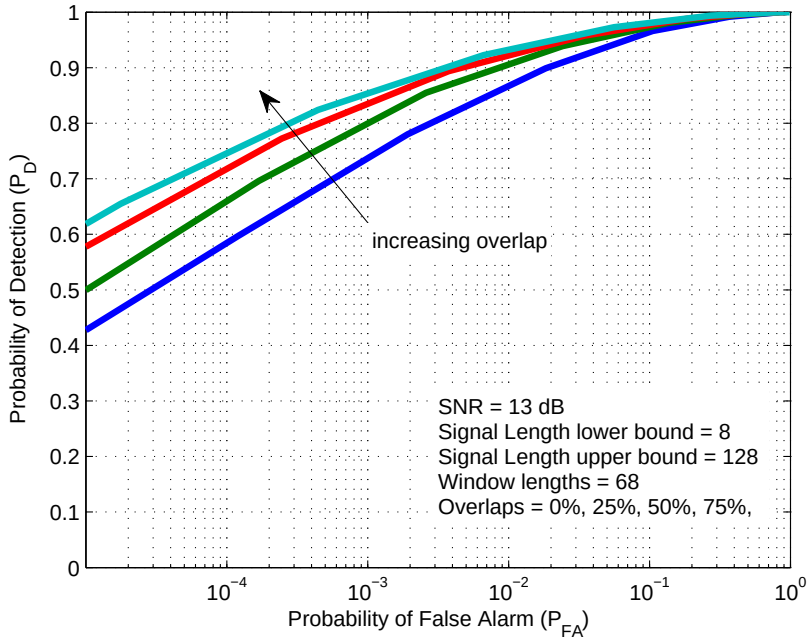

Figure 5.7: Performance for overlapping single window detector

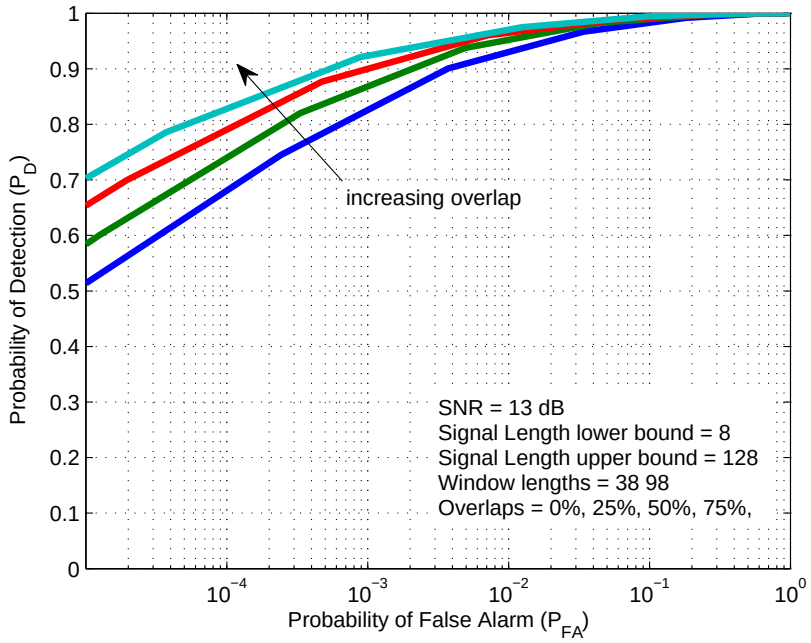

Figure 5.8: Performance for overlapping two window detector

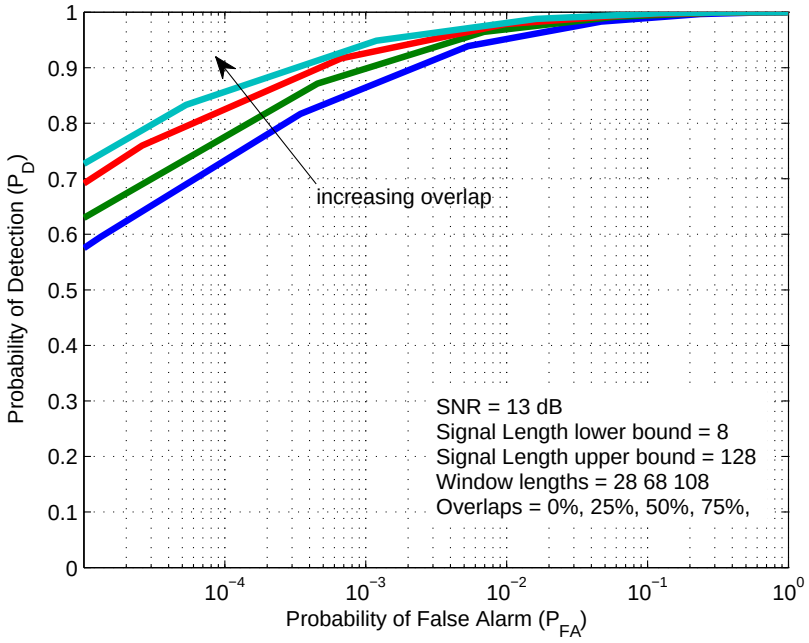

Figure 5.9: Performance for overlapping three window detector

CHAPTER 6

CONCLUSION

In this thesis, binary hypothesis testing for signals of unknown length and delay under Gaussian noise is investigated. Detection performances of different scenarios under noise are analyzed. When the length parameter is unknown, a multiple-window detector is used. When the delay time is also unknown, overlapping windows are used. The performance of this detector is analyzed. Simulation results are added.

When multiple windows were used for the random length case, performance increase is noted. This performance increase however depends on the domain of the length parameter. When the shortest and the longest possible signal lengths are very close to each other, a single window detector structure may be preferred. When these two ends are far away however, multiple window structure greatly increases the performance. The structure of the windows and how many to use depends on the specific scenario and available computation power.

6.1 Results

For signals with random length, if window lengths are chosen as their optimal values, multiple window detectors give a better performance when their number of windows are increased. A rigourious proof for this statement is not given, but generally it is believed to be true. The GLRT detector derived for the random length case, and the results of some simulations support this idea.

For signals with random initial times, overlapping windows are used. Simulations gave clear results that increasing overlaps gives better performance. This idea is consistent with the derived GLRT detector for random delay.

In order to find simple detectors having analytical forms, GLRT detectors are derived. In GLRT detectors, signal parameters are estimated and the estimated values are used in the detector as if they are the actual values. By this procedure detection and estimation are performed at the same time. Noise paremeters however are assumed to be known throughout the work. When the noise parameters are unknown, those parameters also have to be estimated. For example, the cell averaging constant false alarm method is a good method to adjust thresholds adaptively according to changing noise parameters [40]. However, estimating the noise parameters when they are unknown is out of the scope of this work.

6.2 Future Work

For a given detector, estimating the probability of false alarms for very small values by simulation usually takes very long time. The reason is that one needs to repeat the experiment for many times to see the effects of that very small pfa value. Therefore theoretical false alarm calculations are critical for properly setting the threshold values and for evaluating the performance of the detector. Some of the future work will be about those probability of false alarm calculations.

For the detector derived for the random length case, probability of false alarm calculations for lengths greater than 4 contain a number of integrals to be numerically computed. A work will be carried to simplify the forms for the relations.

There does not exist theoretical probability of false alarm and detection calculations for the overlapping window detectors. Exact forms or some approximations will be tried to be calculated.

For the multiple window detectors, a formula is suggested to set window lengths to give a performance close to optimal. A work will be carried out to find an optimal method of choosing the window lengths.

REFERENCES

[1] J.R. Gabriel and S.M. Kay. On the relationship between the GLRT and UMPI tests for the detection of signals with unknown parameters. *Signal Processing, IEEE Transactions on*, 53(11):4194–4203, 2005.

[2] Harry L. Van Trees. *Detection, Estimation, and Modulation Theory, Part I*. Wiley-Interscience, 1 edition, September 2001.

[3] Harry L. Van Trees. *Nonlinear Modulation Theory*. Wiley-Interscience, December 2002.

[4] Harry L. Van Trees. *Radar-Sonar Signal Processing and Gaussian Signals in Noise*. Wiley-Interscience, 1 edition, September 2001.

[5] Louis Scharf. *Statistical Signal Processing*. Prentice Hall, 1 edition, April 1990.

[6] Steven M. Kay. *Fundamentals of Statistical Signal Processing, Volume I: Estimation Theory*. Prentice Hall, 1 edition, April 1993.

[7] Steven M. Kay. *Fundamentals of Statistical Signal Processing, Volume 2: Detection Theory*. Prentice Hall, 1 edition, February 1998.

[8] H. Vincent Poor. *An Introduction to Signal Detection and Estimation*. Springer, 2nd edition, March 1994.

[9] Carl W. Helstrom. *Elements of Signal Detection and Estimation*. Prentice Hall, August 1994.

[10] Bernard C. Levy. *Principles of Signal Detection and Parameter Estimation*. Springer US, Boston, MA, 2008.

[11] W.A. Gardner. Signal interception: a unifying theoretical framework for feature detection. *Communications, IEEE Transactions on*, 36(8):897–906, 1988.

[12] L. Izzo, L. Paura, and M. Tanda. Signal interception in non-Gaussian noise. *Communications, IEEE Transactions on*, 40(6):1030–1037, 1992.

[13] F. Gini, A. Farina, and M. Greco. Selected list of references on radar signal processing. *Aerospace and Electronic Systems, IEEE Transactions on*, 37(1):329–359, 2001.

[14] Francois Le Chevalier. *Principles of Radar and Sonar Signal Processing*. Artech House Publishers, 1st edition, March 2002.

[15] G. Turin. An introduction to matched filters. *Information Theory, IRE Transactions on*, 6(3):311–329, 1960.

[16] H. Urkowitz. Energy detection of unknown deterministic signals. *Proceedings of the IEEE*, 55(4):523–531, 1967.

[17] V.I. Kostylev. Energy detection of a signal with random amplitude. In *Communications, 2002. ICC 2002. IEEE International Conference on*, volume 3, pages 1606–1610 vol.3, 2002.

[18] J.E. Salt and H.H. Nguyen. Performance prediction for energy detection of unknown signals. *Vehicular Technology, IEEE Transactions on*, 57(6):3900–3904, 2008.

[19] Janne Lehtomäki. *Analysis of Energy Based Signal Detection*. PhD thesis, University of Oulu, Oulu, 2005.

[20] J. Williams and G. Ricker. Signal detectability performance of optimum fourier receivers. *Audio and Electroacoustics, IEEE Transactions on*, 20(4):264–270, 1972.

[21] B.H. Maranda. On the false alarm probability for an overlapped FFT processor. *Aerospace and Electronic Systems, IEEE Transactions on*, 32(4):1452–1456, 1996.

[22] M.M. Nayegi, M.R. Aref, and M.H. Bastani. Detection of coherent radar signals with unknown doppler shift. *Radar, Sonar and Navigation, IEE Proceedings -*, 143(2):79–86, 1996.

[23] L. Vergara, J. Moragues, J. Gosálbez, and A. Salazar. Detection of signals of unknown duration by multiple energy detectors. *Signal Processing*, 90(2):719–726, February 2010.

[24] A. P. Trifonov, V. I. Parfenov, and D. V. Mishin. Optimum reception of a signal with unknown duration against the background of white noise. *Radiophysics and Quantum Electronics*, 40(12):1031–1038, 1997.

[25] Saleem A. Kassam. *Signal Detection in Non-Gaussian Noise*. Springer, 1 edition, December 1987.

[26] D. Sengupta and S.M. Kay. Parameter estimation and GLRT detection in colored non-Gaussian autoregressive processes. *Acoustics, Speech and Signal Processing, IEEE Transactions on*, 38(10):1661–1676, 1990.

[27] Jorge Moragues, Luis Vergara, Jorge Gosalbez, and Ignacio Bosch. An extended energy detector for non-Gaussian and non-independent noise. *SIGNAL PROCESSING*, 89(4):656–661, APR 2009.

[28] K.R. Kolodziejski and J.W. Betz. Detection of weak random signals in IID non-Gaussian noise. *Communications, IEEE Transactions on*, 48(2):222–230, 2000.

[29] G.B. Giannakis and M.K. Tsatsanis. Signal detection and classification using matched filtering and higher order statistics. *Acoustics, Speech and Signal Processing, IEEE Transactions on*, 38(7):1284–1296, 1990.

[30] B.M. Sadler, G.B. Giannakis, and Keh-Shin Lii. Estimation and detection in non-Gaussian noise using higher order statistics. *Signal Processing, IEEE Transactions on*, 42(10):2729–2741, 1994.

[31] C. Khatri and C.R. Rao. Effects of estimated noise covariance matrix in optimal signal detection. *Acoustics, Speech and Signal Processing, IEEE Transactions on*, 35(5):671–679, 1987.

[32] Xiu-Ying Hou, N. Morinaga, and T. Namekawa. Direct evaluation of radar detection probabilities. *Aerospace and Electronic Systems, IEEE Transactions on*, AES-23(4):418–424, 1987.

[33] D.A. Shnidman. Radar detection probabilities and their calculation. *Aerospace and Electronic Systems, IEEE Transactions on*, 31(3):928–950, 1995.

[34] Athanasios Papoulis. *Probability, Random Variables and Stochastic Processes*. McGraw-Hill Companies, 3rd edition, February 1991.

[35] F. Liese and Klaus-J. Miescke. *Statistical Decision Theory: Estimation, Testing, and Selection*. Springer, 1 edition, June 2008.

[36] Mark A. Richards. *Fundamentals of Radar Signal Processing*. McGraw-Hill, 1 edition, June 2005.

[37] Marvin K. Simon. *Probability Distributions Involving Gaussian Random Variables: A Handbook for Engineers and Scientists*. Springer, November 2006.

[38] F.J. Harris. On the use of windows for harmonic analysis with the discrete fourier transform. *Proceedings of the IEEE*, 66(1):51–83, 1978.

[39] A. Nuttall. Some integrals involving the Q_M function (Corresp.). *Information Theory, IEEE Transactions on*, 21(1):95–96, 1975.

[40] P.P. Gandhi and S.A. Kassam. Optimality of the cell averaging CFAR detector. *Information Theory, IEEE Transactions on*, 40(4):1226–1228, 1994.